بسم الله الرحمن الرحيم

Sudan University of Science and Technology

Collage of Graduate Studies

M.sc in biomedical engineering

A research title:

Speckle noise reduction in ultrasound images using modified hybrid median filter

عنوان البحث:

الحد من ضوضاء الرقطة في صور الموجات فوق الصوتية بإستخدام مرشح متوسط الهجين المعدل

Represented by:

Razan Ibrahim Al Sharif.

Supervisor:

Dr. Banazier Ahmed Abrahim.

April (2019)

الآيـــة

قال الله تعالى:

(قُلْ هَلْ يَسْتَوِي الَّذِينَ يَعْلَمُونَ وَالَّذِينَ لَا يَعْلَمُونَ إِنَّمَا يَتَذَكَّرُ أُولُو الْأَلْبَابِ)

(9) الزمر

Dedication

This project dedicated to my beloved parents,
Who educated me and enabled me to reach this level.

Acknowledgment

Thanks to Allah at first ,and would like to express gratitude to my supervisor Dr.Banazier Ahmed Abrahim for all helping guidance, her patience valuable encouragement during this study .Also would like to express thanks to the staff members at Sudan University, department of biomedical engineering. Also, heartily thankful our teachers and friends whose support us in this project.

Abstract:

Ultrasound imaging is a widely used in medical diagnosing imaging techniques. Because of following: low cost, painless and considered harmless to the patients.

However, the main problem facing ultrasound images is speckle noise, which is inherent multiplicative noise that reduces the overall quality of the images in term of resolution and contrast.

Edge detection in medical image is an important task for object recognition of the human organs, and it is an essential pre-processing step in medical image segmentation and 3D reconstruction. Successful results of image analysis extremely depend on edge detection. Up to now many edge detection methods have been developed. But, they are sensitive to noise.

So, this thesis proposes, a new method of speckle noise reduction with ability to enhancing image edges, i.e. a modified version of hybrid median filter, it works in sub-windows and it is divided it vertical, horizontal and diagonal regions. Then it computes the mean and the median value of diagonals element, and maximum of vertical and horizontal elements in a moving window. After that the two values are compared with the central pixel and the median value of the three values will be the new pixel value. Ultimately six edge detection techniques were applied using Proposed Method and hybrid median filter images.

The experimental result shows that by modifying the hybrid median filter, and combining it with Roberts edge detection operator this gives better edge preserving characteristics than hybrid median filter, edge detection helps in extracting useful features for pattern recognition. and the proposed method is highly effective in noise separation on compression other filters using image quality evaluation metrics.

المستخلص:

التصوير بالموجات فوق الصوتيه شائع الاستخدام في التصوير الطبي التشخيصي وذلك، لأنه قليل التكلفة، عديم الألم وكما يعتبر غير ضار بالمرضى. المشكلة الأسايسة التى تواجه التصوير بالموجات فوق الصوتية هي ضوضاء الرقطة، وهي ضوضاء متأصله في الصورة وتقلل من الجوده الكلية من حيت التباين والوضوح.

الكشف عن الحواف في الصورة تؤدي دورا هاما في التعرف على الأعضاء البشرية وتمييزها، إذ يعد خطوة ما قبل المعالجة الأساسية في عملية تحليل الصورالطبية و تجزئتها واستخلاص معلومات معينة منها وإعادة بناء الصور ثلاثية الابعاد. تم تطويرالعديد من أساليب الكشف عن الحافة التي أثبتت كفاءتها في مجالات معينة وأعطت نتائج جيدة عند تطبيقها .ولكن تتمحور مشكلة هذه التقنيات في حساسيتها للضوضاء.

لذلك، هذه الأطروحة تقترح طريقة جديده للتقليل من ضوضاء الرقطه مع إمكانية تحسين حواف الصورة. ان هذه الطريقة تعمل في نافذه جزئية تقوم بتقسيم الصورة الى مناطق رأسية وأفقية، ومناطق قطرية.

وبعد ذلك تقوم بحساب كل من الوسط والوسيط لعناصر القطر والقيمة القصوى للعناصر الأفقية والرأسية في النافذة المتحركة. أخيرا تقوم بمقارنة القيمتين مع بكسل الوسط ومن ثم أخد القيمه المتوسطة واعتبارها البكسل الجديد. اخيرا، تم تطبيق سته من طرق كشف الحواف على صورتي مرشح المتوسط الهجين المعدل ومرشح المتوسط الهجين.

نتائج التجارب أوضحت أن بعد تعديل مرشح المتوسط الهجين ودمجه مع طريقة روبرتز لكشف الحواف، هذا يعطي اداء افضل في الحفاظ على الحواف من ذلك الأداء في مرشح المتوسط الهجين. الكشف عن الحواف يساعد على استخراج مميزات مفيدة للتعرف على الأنماط. كما أن الطريقة المقترحة هي طريقة فعالة في فصل الضوضاء إذا ماتمت مقارنتها ببعض مرشحات ازالة ضوضاء الرقطة من مقاييس تقييم جودة الصورة.

Table of contents

Chapter Three

Literature review

Chapter Four

List of Figures

List of Tables

Abbreviation

US	Ultrasound
US	B-mode Ultrasound Brightness mode
US	A-mode Ultrasound Amplitude mode
US	M-mode Ultrasound Motion mode
SND	Scatter Number Density
FFS	Fully Formed Speckle pattern
NRLR	Non Randomly distributed with Long-Range order
NRSR	Non Randomly distributed with Short-Range order
PDF	Probability Density Function
PZT	Piezoelectric
PVDF	Poly vinyli denedi fluoride
CMUT	Capacitive micro machined ultrasonic transducer
DsFgf4d	Geometric Filter
DsFls	Linear scaling gray level filter
SRAD	Speckle reduction anisotropic diffusion
HMF	Hybrid Median Filter

PDE	Partial Differential Equation
TVD	Total Variation Denoising Filters
RMSE	Root Mean Square Error
SNR	Signal to Noise Ratio
PSNR	Peak Signal to Noise Ratio
SSIM	Structural Similarity Index
UIQI	Universal Image Quality Index
EPF	Edge Preserving Factor
MHMF	Modified Hybrid Median Filter

CHAPTER ONE

1.1 General review

Medical images are usually corrupted by noise in its acquisition and Transmission. The main objective of Image denoising techniques is necessary to remove such noises while retaining as much as possible the important signal features. [1]

Ultrasonic imaging is a widely used medical imaging procedure because it is economical, comparatively safe, transferable, and adaptable. Though, one of its main shortcomings is the poor quality of images, which are affected by speckle noise. The existence of speckle is unattractive since it disgrace image quality and it affects the tasks of individual interpretation and diagnosis. [2]

Accordingly, speckle filtering is a central pre-processing step for feature extraction, analysis, and recognition from medical imagery measurements. Previously a number of filters have been proposed for speckle mitigation. An appropriate method for speckle reduction is one which enhances the signal to noise ratio while conserving the edges and lines in the image.[3]

Edges are one of the most important elements in image analysis and computer vision, because they play quite a significant role in many applications of medical image processing, in particular for segmentation. A lot of medical image processing methods rely on edge detection as a pre - processing stage. [4]

Medical images edge detection is an important work for object recognition of the human organs such as lungs and ribs, and it is an essential pre-processing step in medical image segmentation. Since edges contain a major function of image information. The function of edge detection is to identify the boundaries of homogeneous regions in an image based on properties such as

intensity and texture, so there are many methods for edge detection; they can be divided into two categories: spatial domain detection and transformational domain detection. [4]

1.2 Problem of the statement

In medical image processing, it is very vital to obtain exact images to facilitate accurate explanation for the known request. Low image quality is an obstacle for effective feature extraction, analysis, recognition and quantitative measurements. Therefore, there is a fundamental need of noise reduction from medical images without affecting important image features such as edges.

1.3 General objective

Give an overview about speckle noise, how to generate, has properties, and what the effectiveness of it on the ultrasound image, therefor design a modified hybrid median filter with edge detection for speckle noise reduction in ultrasound image.

1.4 Specific objectives

A- Learn about types of speckle reduction techniques in ultrasound imaging.
B- To carry out a comparative evaluation of despeckling filtering based on image evaluation metrics.
C- Propose new methods as a despeckle filter called Modified Hybrid Media filter.
D- Enhance the edges of an image and use quality evaluation to measure the performance.
E- Carry out a comparative evaluation between Modified Hybrid Media filter and Hybrid Media filter and in term of edge preserving.

1.5 methodology

Images from The Children`s Hospital of Philadelphia database of fetal ultrasound image, and IBE Tech (Giza.Egypt) database of ultrasound Liver image. In the

quantitative study, add speckle noise with different variance on ultrasound images and using a most importantly techniques to removing that noise.

A- Modified Hybrid Median Filter

This proposed filter is the modified version of the hybrid median filter. It works on the sub windows similar to hybrid median filter. The **mean** and **median** values of diagonal pixels is calculated and compared with the **maximum** value of vertical and horizontal pixel in the sub windows and the central pixel. And the **median** value of that set are then saved as the new pixel value

B- Edge detection:

In this section six techniques were applied, detection operators were used (canny, sobel , prewitt , zero-cross, roberts and laplacian of guassian) It has been talk about them in detail in Chapter four. and compute image quality evaluation metrics to evaluated the result and chose best edge operator.

1.6 thesis layout

The layout of this thesis consist of seven chapters; **chapter one;** include introduction, while **chapter two** involve theoretical background, literature review in **chapter three**, in **chapter four** speckle noise and despeckle filter and edge detection methods, in **chapter five** materials and method description , however in **chapter six** the results and discussions were viewed , finally **chapter seven** is conclusion and future work.

CHAPTER TWO

2.1 Introduction

Ultrasound or ultrasonography is a medical imaging technique that uses high frequency sound waves and their echoes, Known as a "*pulse echo technique*". The technique is similar to the echolocation used by bats, whales and dolphins, as well as **SONAR** used by submarines etc. Medical imaging is an important source of diagnosing the malfunctions inside human body. Some crucial Medical imaging instruments are X-ray, Ultrasound, Computed Tomography (**CT**), and Magnetic Resonance Imaging (**MRI**). Medical ultrasound imaging is one of the common techniques in detecting and visualizing the hidden body parts. [5].

There could be distortions due to improper contact or air gap between the transducer probe and the human body. Another kind of distortion that may occur during ultrasound imaging is due to the beam forming process and also during the signal processing stage. In order to overcome through various distortions, image processing has been successfully used. Image processing is a significant technique in medical field, especially in surgical decisions.[5]

Converting an image into homogeneous regions has been an area of hot research from a decade, especially when the image is made up of complex textures. Various techniques have been proposed for this task, including spatial frequency techniques. Image processing techniques have been used widely depending on the specific application and image modalities. Computer based detection of abnormal growth of tissues in a human body are preferred to manual processing methods in the medical investigations because of accuracy and satisfactory results. Several methods for processing the ultrasound images have been developed. [5]

2.2 Basics of ultrasound

Ultrasound is sound with a frequency above the audible range which ranges from 20 Hz to 20 kHz. Sound is mechanical energy that needs a medium to propagate. Thus, in contrast to electromagnetic waves, it cannot travel in vacuum.

The frequencies normally applied in clinical imaging lies between 1 MHz and 20 MHz. The sound is generated by a transducer that first acts as a loudspeaker

sending out an acoustic pulse along a narrow beam in a given direction. The transducer subsequently acts as a microphone in order to record the acoustic echoes generated by the tissue along the path of the emitted pulse. These echoes thus carry information about the acoustic properties of the tissue along the path. The emission of acoustic energy and the recording of the echoes normally take place at the same transducer, in contrast to CT imaging, where the emitter (the X-ray tube) and recorder (the detectors) are located on the opposite side of the patient [6].

Ultrasound (as well as sound) needs a medium, in which it can propagate by means of local deformation of the medium. One can think of the medium as being made of small spheres (*e.g.* atoms or molecules), that are connected with springs. When mechanical energy is transmitted through such a medium, the spheres will oscillate around their resting position. Thus, the propagation of sound is due to a continuous interchange between kinetic energy and potential energy, related to the density and the elastic properties of the medium, respectively. [6].

The two simplest waves that can exist in solids are *longitudinal* waves in which the particle movements occur in the same direction as the propagation (or energy flow), and *transversal* (or *shear* waves) in which the movements occur in a plane perpendicular to the propagation direction. In water and soft tissue the waves are mainly longitudinal. The frequency, $\mathcal{F}$, of the particle oscillation is related to the wavelength, λ, and the propagation velocity c:

$$\lambda \mathcal{F} = c \qquad (2.1)$$

The sound speed in soft tissue at 37°C is around 1540 m/s, thus at a frequency of 7.5 MHz, the wavelength is 0.2 mm[6].

2.3Types of ultrasound waves:

Two simple waves, both are theoretical, since they need an infinitely large medium.

Since optical rays can be visualized directly, and since they behave in a manner somewhat similar to acoustic waves, they can help in understanding reflection, scattering and other phenomena taking place with acoustic waves. Therefore, there will often be made references to optics.

There are two types of waves that are relevant. They can both be visualized in 2D with a square acrylic water tank placed on an overhead projector:

- The plane wave which can be observed by shortly lifting one side of the container.
- The spherical wave, which can be visualized by letting a drop of water fall into the surface of the water.

When the plane wave is created at one side of the water tank, one will also be able to observe the reflection from the other side of the tank. The wave is reflected exactly as a light beam from a mirror or a billiard ball bouncing off the barrier of the table.

The spherical wave, that on the other hand, originates from a point source and propagates in all directions; it creates a complex pattern when reflected from the four sides of the tank[6].

2.4 The generation of ultrasound

2.4.1 Mainstream technologies

In this section, the state of the art in the mainstream technologies which underpin the contemporary clinical applications of ultrasonic imaging is reviewed. The range of these technologies is now so great that it has been necessary to be selective in choosing those technologies which seem to be most important; it is hoped that this selection will not be thought to be too biased [7].

2.4.2Transducers

In some respects, the transducer is the most critical component in any ultrasonic imaging system. In other words, such is the state of the art in systems such as electronic circuitry and display technology that it is the performance of the transducer which determines how closely the limits imposed by the characteristics of the tissues themselves can be approached.

Nowadays, the transducers which are in clinical use almost exclusively use a piezoelectric material, of which the artificial ferroelectric ceramic, lead zircon atetitanate (PZT) is the most common. The ideal transducer for ultrasonic imaging would have a characteristic acoustic impedance perfectly matched to that of the

(human) body; have high efficiency as a transmitter and high sensitivity as a receiver, a wide dynamic range and a wide frequency response for pulse operation. PZT has a much higher characteristic impedance than that of water but it can be made to perform quite well by the judicious use of matching layers consisting of materials with intermediate characteristic impedances. Even better performance can be obtained by embedding small particles or shaped structures of PZT in a plastic to form a composite material: this has lower characteristic impedance than that of PZT alone, although it has similar ferroelectric properties [7].

Poly vinyli denedi fluoride (PVDF) is a plastic which can be polarized so that it has piezoelectric properties. The piezoelectric effect can be enhanced by the addition of small quantities of appropriate chemicals. The advantages of this material are that it has a relatively low characteristic impedance and broad frequency bandwidth; it is fairly sensitive as a receiver but rather inefficient as a transmitter. Piezoelectric transducers are normally operated over a band of frequencies centered at their resonant frequency. The resonant frequency of a transducer occurs when it is half a wavelength in thickness. Typically, a PZT transducer resonant at a frequency of, say, 3 MHz is about 650 μm thick and this means that it is sufficiently mechanically robust for simple, even manual, fabrication techniques to be employed in probe construction. Higher frequency transducers are proportionally thinner and, consequently, more fragile.

The potential of capacitive micro machined ultrasonic transducers (CMUTs) at least partially to replace PZT and PVDF devices in ultrasonic imaging is the subject of current research. A CMUT consists of a micro machined capacitor, typically mounted on a silicon substrate and with a thin electroded membrane as the other plate of the capacitor: these acts as the active surface of the transducer. A dc voltage is applied between the plates of the device; the application of an AC voltage causes the membrane to transmit a corresponding oscillatory force, while a received wave causes a corresponding change in the spacing between the plates, thus generating an electrical signal. CMUTs are adequately sensitive as receivers, but need high voltages to be effective transmitters. Some of the potential advantages of these devices are that they can be fabricated into arrays with integrated electronics and, if manufactured in large quantities, could be relatively inexpensive.[7]

Although some simple probes contain single-element transducers (e.g., one element for transmitting and one for receiving, in a continuous-wave Doppler system), most modern imaging systems use arrays of transducer elements for beam forming [7].

2.4.3Piezoelectricity

The acoustic field is generated by using the piezo electric effect present in certain ceramic materials. Electrodes (e.g. thin layers of silver) are placed on both sides of a disk of such a material. One side of the disk is fixed to a damping so-called backing material, the other side can move freely. If a voltage is applied to the two electrodes, the result will be a physical deformation of the crystal surface, which will make the surroundings in front of the crystal vibrate and thus generate a sound field. If the material is compressed or expanded, as will be the case when an acoustic wave impinges on the surface, the displacement of charge inside the material will cause a voltage change on the electrodes; this is used for emission and reception of acoustic energy, respectively [7].

2.5 Beam forming

In ultrasonic imaging, the beam may be scanned through the tissue either by mechanical movement of a single element or an annular array transducer, or by electronic control of a transducer array consisting of a number of small elements. For two-dimensional scanning, the array typically consists of 256 elements. The simplest arrangement is a linear array, within which an aperture is formed from, say, 16 contiguous elements and which is stepped along the array element by element to acquire an image with, in this example, 241 lines.

The same number of lines in a sector format can be acquired by curving the array into a segment of a cylinder. A sector scan can also be acquired by controlling the phases of the signals associated with each of the elements in the aperture. Whatever the arrangement, the application of distinct time delays to excite each element focuses the transmitted beam at a particular range. By transmitting several beams in the same position but with different foci, a sharply focused transmitted beam can be synthesized. On reception, the focus can be swept along the beam by dynamically changing the time delays associated with the active transducer elements, so that its position coincides continuously with that of the instantaneous

origin of the echoes. Both when transmitting and receiving, the amplitudes of the signals associated with the active elements can be weighted to minimize the amplitudes of the beam side lobes, which are critical in determining the image contrast resolution. Also, the number of elements in the active aperture can be dynamically increased with increasing depth of penetration to maintain a constant f number, within the limit imposed by the total length of the array and optimized to minimize the effect of tissue inhomogeneity.[7]

For three-dimensional imaging, the two-dimensional scan plane produced by a one-dimensional linear, curved or phased array can be swept mechanically, either linearly in the orthogonal direction or through a sector. Recently, two-dimensional transducer arrays have been developed. Because of the very large number of transducer elements in these arrays, beam forming in three dimensions can be achieved more economically but with some degradation in performance by sparsely populating the array.[7]

For real-time three-dimensional scanning, several transmitting beams can be synthesized simultaneously; a single receiving beam can be associated with each transmitting beam, or, by increasing the width of each transmitting beam, several sharply focused receiving beams can be accommodated simultaneously in each transmitted beam.

The beam-forming time delays and aperture apodization functions are digitally controlled.

The sampling frequency has to be at least twice the highest ultrasonic frequency, in order to avoid aliasing. Further improvement can be obtained by applying a finite impulse response digital filter or by demodulating the radio-frequency signals to baseband to obtain quadrature signals so that the associated time delays can be finely adjusted by phase rotation.[7]

An intriguing development in high-speed imaging has recently been brought about by the application of limited diffraction beams. A limited diffraction beam can be produced by appropriate excitation of a transducer array. Following the transmission of a single plane wave pulse, the received signals are weighted with limited diffraction beams simultaneously to produce multiple A-lines which can be used to create a complete two-dimensional image [7].

2.6 Ultrasound's interaction with the medium

The interaction between the medium and the ultrasound emitted into the medium can be described by the following phenomena:

The echoes that travel back to the transducer and thus give information about the medium is due to two phenomena: *reflection* and *scattering*. Reflection can be thought of as when a billiard ball bounces off the barrier of the table, where the angle of reflection is identical to the angle of incidence. Scattering (Danish: *spredning*) can be thought of, when one shines strong light on the tip of a needle: light is scattered in all directions. In acoustics, reflection and scattering is taking place when the emitted pulse is travelling through the interface between two media of different acoustic properties, as when hitting the interface of an object with different acoustic properties.[7]

Specifically, reflection is taking place when the interface is large relative to the wavelength (*e.g.* between blood and intima in a large vessel). Scattering is taking place when the interface is small relative to the wavelength (*e.g.* red blood cell).

The abstraction of a billiard ball is not complete, however: In medical ultrasound, when reflection is taking place, typically only a (small) part of the wave is reflected. The remaining part is *transmitted* through the interface. This transmitted wave will nearly always be *refracted*, thus typically propagating in another direction. The only exception is when the wave impinges perpendicular on a large planar interface: The reflected part of the wave is reflected back in exactly the same direction as it came from (like with a billiard ball) and the refracted wave propagates in the same way as the incident wave.[7]

Reflection and scattering can happen at the same time, for instance, if the larger planar interface is rough. The smoother, the more it resembles pure reflection (if it is completely smooth, *specular reflection* takes place). The rougher, the more it resembles *scattering*.

When the emitted pulse travels through the medium, some of the acoustic (mechanical) energy is converted to heat by a process called *Absorption*. Of course, also the echoes undergo absorption.

Finally, the loss in intensity of the forward propagating acoustic pulse due to reflection, refraction, scattering and absorption is under one named *attenuation* [7].

2.6.1 Reflection

The reflection of ultrasound pulses by structures within the body is the interaction that creates the ultrasound image. The reflection of an ultrasound pulse occurs at the interface, or boundary, between two dissimilar materials, as shown in the following figure. In order to form a reflection interface, the two materials must differ in terms of a physical characteristic known as acoustic impedance Z. Although the traditional symbol for impedance, Z, is the same symbol used for atomic number, the two quantities are in no way related. Acoustic impedance is a characteristic of a material related to its density and elastic properties. Since the velocity is related to the same material characteristics, a relationship exists between tissue impedance and ultrasound velocity. The relationship is such that the impedance, Z, is the product of the velocity, v, and the material density, Y, which can be written as:

$$\text{Impedance} = (Y)\,(v) \qquad (2.2)$$

The Production of an Echo and Penetrating Pulse at a Tissue Interface At most interfaces within the body, only a portion of the ultrasound pulse is reflected. The pulse is divided into two pulses, and one pulse, the echo, is reflected back toward the transducer and the other penetrates into the other material, as shown in the above figure. The brightness of a structure in an ultrasound image depends on the strength of the reflection, or echo. This in turn depends on how much the two materials differ in terms of acoustic impedance. The amplitude ratio of the reflected to the incident pulse is related to the tissue impedance values by

$$\text{Reflection loss (dB)} = 20 \log (Z2 - Z1)/(Z2 + Z1) \qquad (2.3)$$

At most soft tissue interfaces, only a small fraction of the pulse is reflected. Therefore, the reflection process produces relatively weak echoes. At interfaces between soft tissue and materials such as bone, stones, and gas, strong reflections are produced [6].

2.6.2 Scattering

While reflection takes place at interfaces of infinite size, scattering takes place at small objects with dimensions much smaller than the wavelength. Just as before, the specific acoustic impedance of the small object must be different from the surrounding medium. The scattered wave will be more or less spherical, and thus propagate in all directions, including the direction towards the transducer. The latter is denoted backscattering.

The scattering from particles much less than a wavelength is normally referred to as Rayleigh scattering. The intensity of the scattered wave increases with frequency to the power of four.

Biologically, scattering can be observed in most tissue and especially blood, where the red blood cells are the predominant cells. They have a diameter of about 7 μm, much smaller than the wavelength of clinical ultrasound [7].

2.6.3 Absorption

Absorption is the conversion of acoustic energy into heat. The mechanisms of absorption are not fully understood, but relate, among other things, to the friction loss in the springs, pure absorption can be observed by sending ultrasound through a viscous liquid such as oil [7].

2.6.4 Attenuation

The Reduction of Pulse Amplitude by Absorption of Its Energy As the ultrasound pulse moves through matter, it continuously loses energy. This is generally referred to as attenuation. Several factors contribute to this reduction in energy. One of the most significant is the absorption of the ultrasound energy by the material and its conversion into heat. Ultrasound pulses lose energy continuously as they move through matter. This is unlike x-ray photons, which lose energy in "one-shot" photoelectric or Compton interactions. Scattering and refraction interactions also remove some of the energy from the pulse and contribute to its overall attenuation, but absorption is the most significant.

The rate at which an ultrasound pulse is absorbed generally depends on two factors: (1) the material through which it is passing, and (2) the frequency of the

ultrasound. The attenuation (absorption) rate is specified in terms of an attenuation coefficient in the units of decibels per centimeter. Since the attenuation in tissue increases with frequency, it is necessary to specify the frequency when an attenuation rate is given. The attenuation through a thickness of material, x is given by:

$$\text{Attenuation (dB)} = (a)\,(f)\,(x) \qquad (2.4)$$

Where (a) is the attenuation coefficient (in decibels per centimeter at 1 MHz), and (f) is the ultrasound frequency, in megahertz [8].

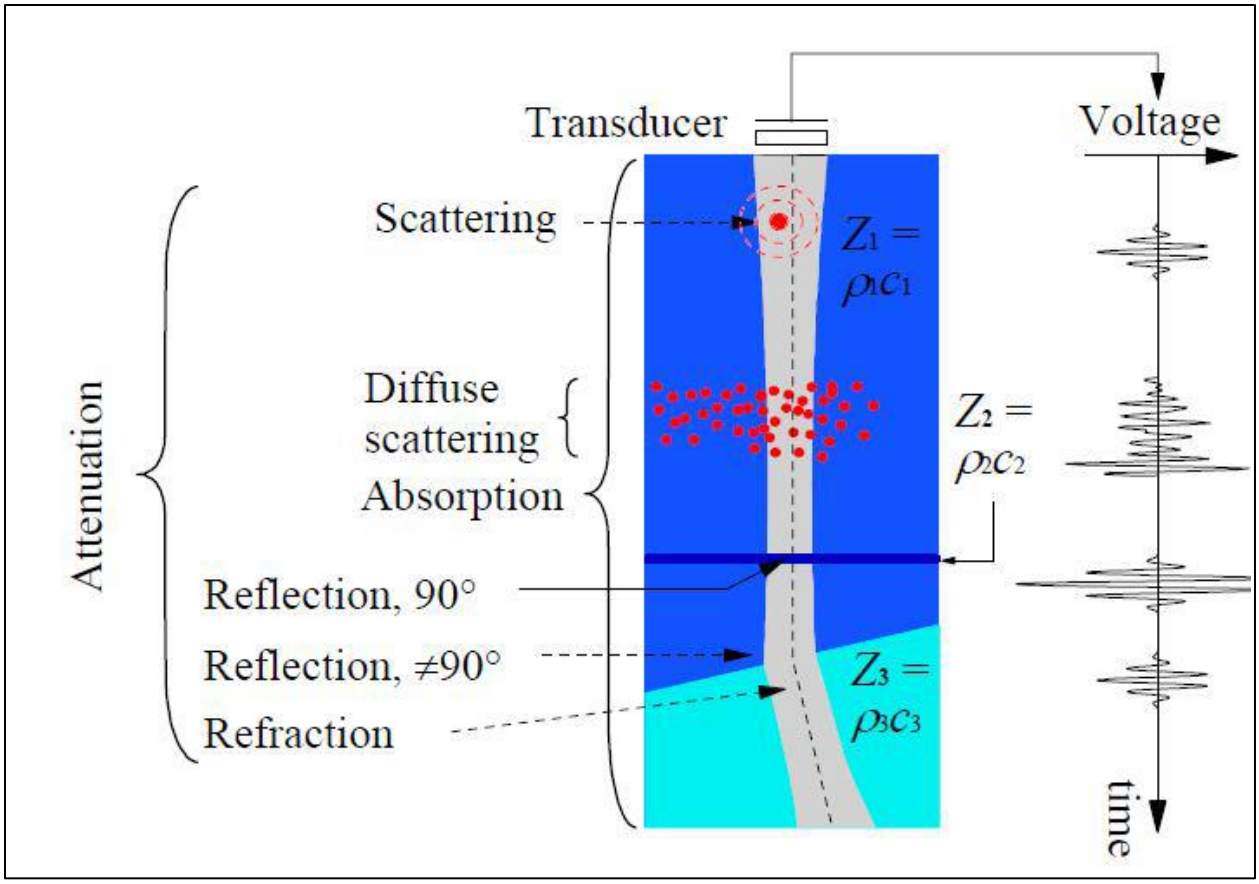

Figure 2.1: sketch of the ultrasound interaction with tissue [7].

2.7 Imaging

The basic principle behind pulse-echo imaging an acoustic pulse is emitted from the transducer, scattered by the point reflector and received after a time interval which is equal to the round trip travel time. The emitted pulse is also present in the received signal due to limitations of the electronics controlling the transducer. Right: the signal processing creating the envelope of the received signal followed by calculation of the logarithm yielding the scan line.

Imaging is based on the pulse-echo principle: A short ultrasound pulse is emitted from the transducer. The pulse travels along a beam pointing in a given direction. The echoes generated by the pulse are recorded by the transducer. This electrical signal is always referred to as the received signal. The later an echo is received, the deeper is the location of the structure giving rise to the echo. The larger the amplitude of the echo received, the larger is the average specific acoustic impedance difference between the structure and the tissue just above. An image is then created by repeating this process with the beam scanning the tissue.

All this will now be considered in more detail by considering how Amplitude mode, Motion mode and Brightness mode work [7].

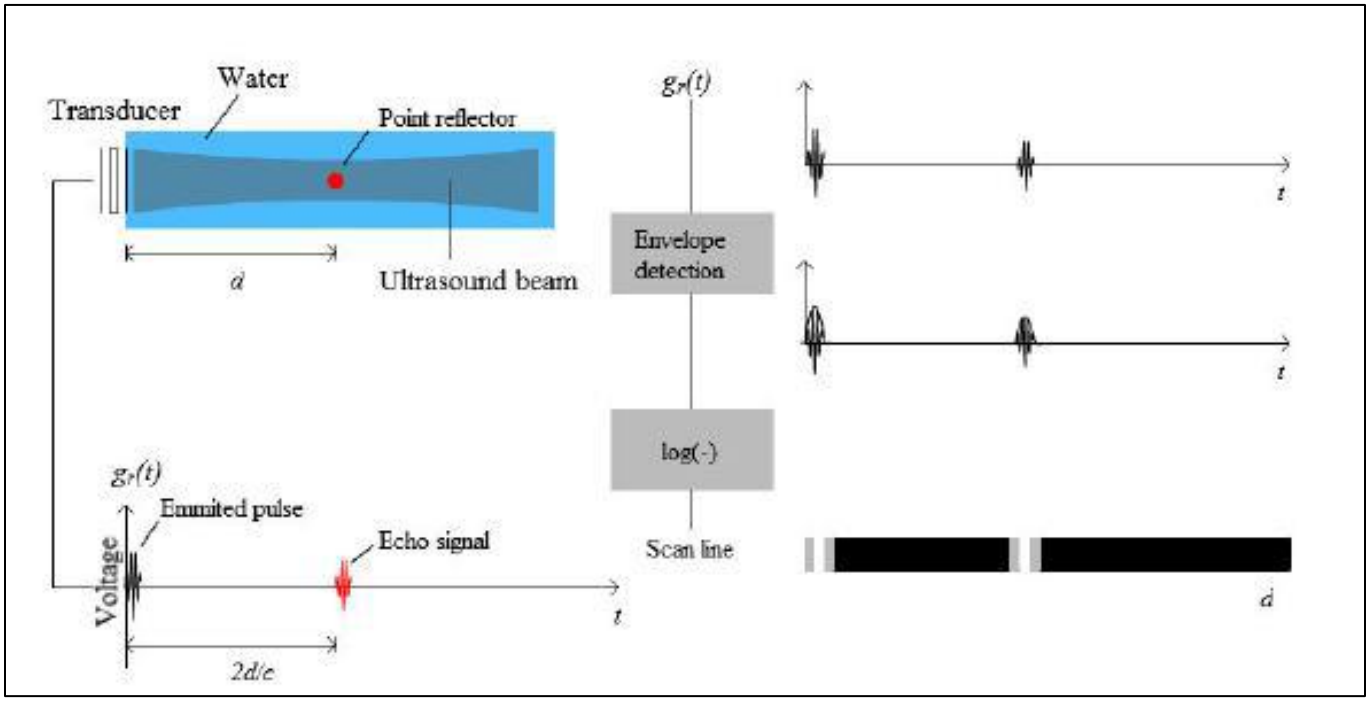

Figure 2.2: illustrate the image forming in ultrasound [5].

There are several options to form an image from this pulse-echo signal:

A-mode

A single point scatterer is located in front of the transducer at depth *d*. A short pulse is emitted from the transducer, and at time 2*d*/c, the echo from the point target is received by the same transducer. Thus, the deeper the point scatterer is positioned, the later the echo from this point scatterer arrives. If many point scatterers (and reflectors) are located in front of the transducer, the total echo can be found by simple superposition of each individual echo, as this is a linear system, when the pressure amplitude is sufficiently low.

The *scan line* is created by calculating the envelope of the received signal followed by calculation of the logarithm, in order to compress the range of image values for a better adoption to the human eye. So, the scan line can be called a *gray scale line*. The M-mode and B-mode images are made from scan lines [6].

M-mode

If the sequence of pulse emission and reception is repeated infinitely, and the scan lines are placed next to each other (with new ones to the right), *motion mode*, or M-mode, is obtained. The vertical axis will be depth in meters downwards, while the horizontal axis will be time in seconds pointing to the right. This mode can be useful when imaging heart valves, because the movement of the valves will make distinct patterns in the "image" [6].

B-mode

Brightness or B-mode is obtained by physically moving the scan line to a number of adjacent locations. The transducer is moved in steps mechanically across the medium to be imaged. Typically 100 to 300 steps are used, with spacing between 0.25λ and 5λ at each step; a short pulse is emitted followed by a period of passive registration of the echo. In order to prevent mixing the echoes from different scan lines, the registration period has to be long enough to allow all echoes from a given emitted pulse to be received [6].

TM-mode:

Time motion diagrams visualize movements of sound-reflecting tissue borders. This mode offers functional rather than morphological inspection [9].

D-mode:

The doppler mode makes use of the doppler effect (i.e., a shift infrequency that occurs if the source of sound, the receptor, or the reflector is moved) in measuring and visualizing blood flow. Several visualization modes are used:

1. Color Doppler: The velocity information is presented as a color coded overlay on top of a B-mode image;

2. Continuous Doppler: Doppler information is sampled along a line through the body, and all velocities detected at each point in time are presented (on a time line).

3. PW Doppler: Pulsed-wave Doppler information is sampled from only asmall sample volume (defined in the 2D B-mode image), and presented on a time line.

4. Duplex: Color and (usually) PW Doppler are simultaneously displayed. [9]

2.8 Importance of ultrasound Imaging

ULTRASOUND imaging application in medicine and other fields is enormous. It has several advantages over other medical imaging modalities. The use of ultrasound in diagnosis is well established because of its noninvasive nature, low cost, capability of forming real time imaging and continuing improvement in image quality. It is estimated that one out of every four medical diagnostic image studies in the world involves ultrasonic techniques. US waves are characterized by frequency above 20 KHz which is the upper limit of human hearing. In medical US applications, frequencies are used between 500 KHz and 30 MHz B-mode imaging is the most used modality in medical US. An US transducer which is placed onto the patient's skin over the imaged region sends an US pulse which travels along a beam into the tissue. Due to interfaces some of the US energy is reflected back to the transducer which converts it into echo signals. These signals are then sent into amplifiers and signal processing circuits in the imaging machine's hardware to

form a 2-D image. This process of sending pulses launched in different directions is repeated in order to examine the whole region in the body. Thus, US imaging involves signals which are obtained by coherent summation of echo signals from scatterers in the tissue. In many cases volume quantification is important in assessing the progression of diseases and tracking progression of response to treatment. Thus, 3D ultrasound imaging has drawn great attention in recent years [10].

2.9 Ultrasound Imaging System

Figure (2.3) shows a functional block diagram of an ultrasound imaging system. The construction of ultrasound B-mode image involves capturing the echo signal returned from tissue at the surface of piezoelectric crystal transducers. These transducers convert the ultrasonic RF mechanical wave into electrical signal. Convex ultrasound probes collect the echo from tissue in a radial form. Each group of transducers is simultaneously activated to look at a certain spatial direction from which they generate a raw line signal (stick) to be used later for raster image construction. These sticks are then demodulated and logarithmically compressed to reduce their dynamic range to suit the commercial display devices. The final Cartesian image is constructed from the sampled sticks in a process called scan conversion.

Speckle reduction techniques can be applied on envelope detected data, log compressed data or on scan converted data. However, slightly different results will be produced for each data. In the compression stage some useful information about the imaged object may be deteriorated or even lost. However, any processing which works with envelope detected data has more information at its disposal and preserves more useful information. Compared to processing the scan converted image, envelope detected data has fewer pixels and thus incurs lower computational cost.

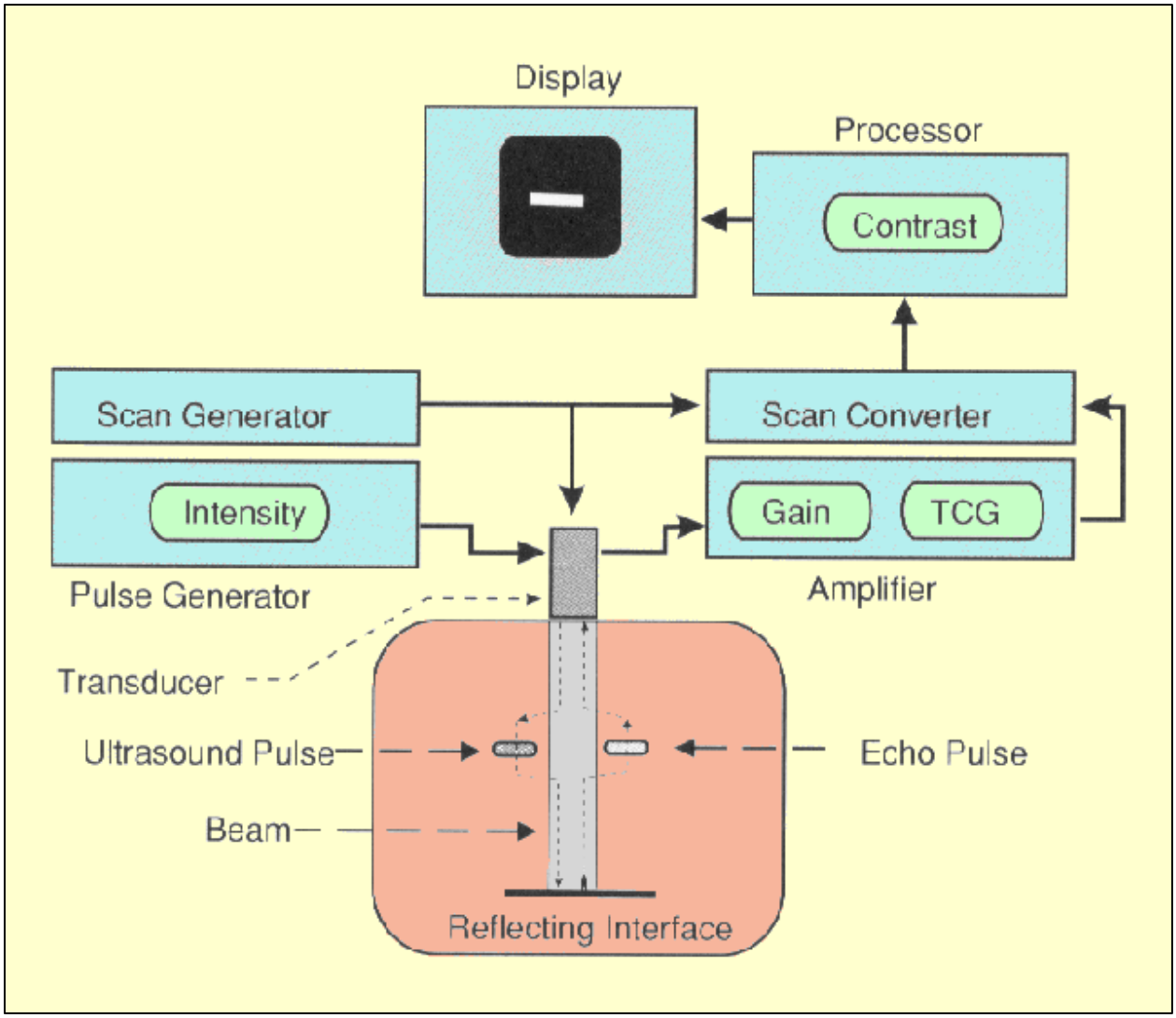

Figure 2.3: Block diagram of Ultrasound Imaging System [8].

For optimum result envelope detected data processing is preferred because some information that lost after the compression stage cannot be recovered by working with logs compressed data or the scan converted image. However, the real time speckle reduction methods are applied on the scan converted image, since the scan converted image is always accessible where most commercial ultrasound systems do not output the envelope detected or log compressed data. [10]

CHAPTER THREE

Literature review

Razan I Elsharif, et. Al.**Wavelet decomposition-based speckle reduction method for ultrasound images by using speckle-reducing anisotropic diffusion and hybrid median (2018**). This paper proposed a new despeckle filter based on hybrid technique to reduce speckle noise from ultrasonic images, by combining Hybrid median filter with SRAD filter. The results demonstrate its higher performance for speckle reduction.

Muhammad S Darus et. al. **Modified hybrid median filter with local preserving for removal of low density random - valued impulse noise in images (2018).** Here a new filter for the removal of random-valued impulse noise in digital gray scale images is presented. The filter is made up of two different stages which is noise detection and filtering steps, in which the properties of the random-valued impulse noise and a modified hybrid median filter i s used.

Jyoti Jaybhay and Rajveer Shastri , **a study of speckle noise reduction filters (June 2015)** , Different filters have been developed as Mean and Median filters, Srad filter. This paper re views filters used to remove speckle noise.

Mehravar et al , **comparison of Different Edge Detections and Noise Reduction on Ultrasound Images of Carotid and Brachial Arteries Using a Speckle Reducing Anisotropic Diffusion Filter(2014 Sep).** This study showed Canny edge detection with SRAD filter is better than other edge detections in terms of speckle suppression and details preservation.

Raman Maini et aI , **Study and Comparison of Various Image Edge Detection Techniques**, in this study the conclude that Canny's edge detection algorithm is computationally more expensive compared to Sobel, Prewitt and Robert's operator. However, the Canny's edge detection algorithm performs better than all these operators under almost all scenarios.

Neha1, D. K. **extended hybrid mean-median filter for image denoising** (2014). In this paper, an enhanced version of hybrid median filter were found as a

combination of mean and median filter. The result shows that the proposed method is performing well comparison to mean, median.

Hussien Ali Hussien, **Software Implementation of Hybrid Median Filter (2013)**, in this paper the algorithm of hybrid median filter is presented and then software is implemented using Matlab package.

Vaishali Kumbhakarna et. Al. **Review on Speckle Noise Reduction Techniques for Medical Ultrasound Image Processing** (2015**).** In this review paper several techniques for effective suppression of speckle noise present in ultrasound images has been studied.

Mustafa,Z. et. Al. **K11. Modified Hybrid Median filter for image denoising (2012).** This work presents a new hybrid median technique denoising algorithm and compared to different denoising techniques. which is a four-step ordering procedure in which pixels from various spatial locations are ordered separately. It has been found that quality evaluation metrics the proposed method performs better than all other methods while still retaining the structural details.

Arpit singhal ,mandeep singh ,**speckle noise removal and edge detection using mathematical morphology(2011)**.In this paper a novel mathematical morphology algorithm is proposed which is use to remove speckle noise from the image and find the edge more efficiently then the previously used edge detector like sobel ,prewitt and canny and filters used to remove speckle noise like LEE and SARD .

R.vanithamani et. Al. **Modified Hybrid Median Filter for Effective Speckle Reduction in Ultrasound Images(2010)**, This paper proposes a statistical filter, which is a modified version of Hybrid Median Filter for speckle Reduction.

S.Kalaivani Narayanan and R.S.D.Wahidabanu, **A View on Despeckling in Ultrasound Imaging, (September 2009),** the objective of this paper is to give an overview about types of speckle reduction techniques in ultrasound imaging.

Ehsan Nadernejad, Mohammad Reza Karami**, Despeckle Filtering in Medical Ultrasound Imaging, (2009)**, this paper proposes filtering techniques for the removal of speckle noise from the image.

Christos P. Loizou and Constantinos S. Pattichis , **Despeckle Filtering Algorithms and Software for Ultrasound Imaging,(2008).** The goal for this book is to introduce the theoretical background (equations), the algorithmic steps, and the MATLAB™ code for the following group of despeckles filters: linear filtering, nonlinear filtering, anisotropic diffusion filtering and wavelet filtering.

CHAPTER FOUR

4.1 Introduction:

Different types of noise. For example, the x-ray images are often corrupted by Poisson noise, while the ultrasound images are affected by **Speckle noise**. Speckle is a complex phenomenon, which degrades image quality with a back scattered wave appearance which originates from many microscopic diffused reflections that passing through internal organs and makes it more difficult for the observer to discriminate fine detail of the images in diagnostic examinations [11].Thus, denoising or reducing these speckle noise from a noisy image has become the predominant step in medical image processing.

4.2 Speckle noise in ultrasound imaging:

Speckle is a form of locally correlated multiplicative noise that corrupts medical ultrasound imaging making visual observation difficult ,Speckle in US B-scans is seen as a granular structure which is caused by the constructive and destructive coherent interference of back scattered echoes from the scatters that are typically much smaller than the spatial resolution of medical ultrasound system. [12]

Speckle is not truly noise in the typical engineering sense since its texture often carries useful information about the image being viewed the speckle are essential information to track features, many cases the speckle noise deteriorates the image quality, degrades the fine details and edge definition.[12]

It also limits the contrast resolution, limiting the detectability of small, low contrast lesions in body. Speckle is always considered as a primary source of medical ultrasound imaging noise, and it should be filtered out without affecting important features of the image.[12]

4.3 Physical Properties and the Pattern of Speckle Noise:

The speckle pattern, which is visible as the typical light and dark spots the image is composed of, results from destructive interference of ultrasound waves scattered from different sites. The nature of speckle has been a major subject of investigation. When a fixed rigid object is scanned twice under exactly the same conditions, one obtains identical speckle patterns. Although of random appearance, speckle is not random in the same sense as electrical noise. However, if the same object is scanned under slightly different conditions, say, with a different

transducer aperture, pulse length, or transducer angulations, the speckle patterns change.[12]

The most popular model adopted in the literature to explain the effects that occur when a tissue is insinuated is illustrated in Figure 3.1, where a tissue may be modeled as a sound absorbing medium containing scatters, which scatter the sound waves. These scatters arise from in homogeneity and structures approximately equal to or smaller in size than the wavelength of the ultrasound, such as tissue parenchyma, where there are changes in acoustic impedance over a microscopic level within the tissue. Tissue particles that are relatively small in relation to the wavelength (i.e., blood cells), and particles with differing impedance that lie very close to one another, cause scattering or speckling.[10]

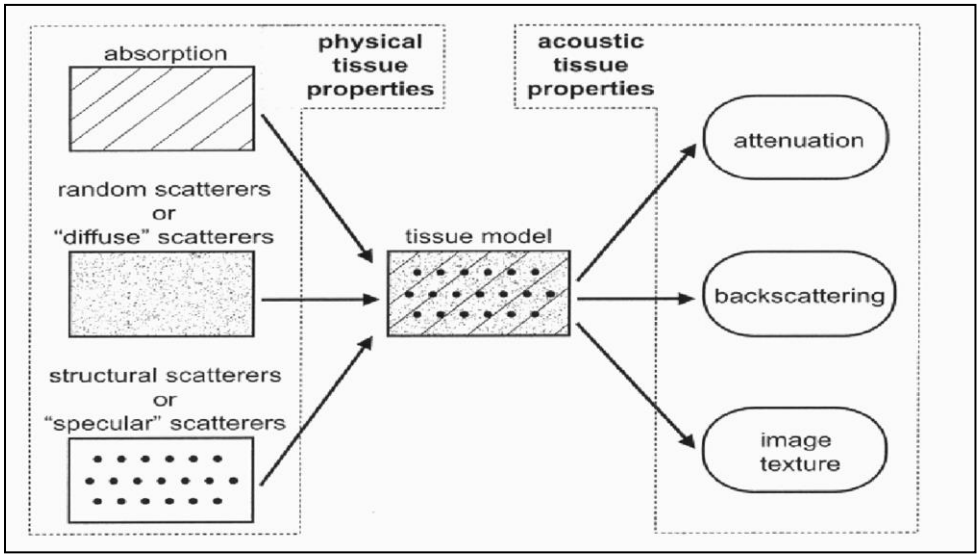

Figure 4.1 the usual tissue model in ultrasound imaging[10]

Absorption of the ultrasound tissue is an additional factor to scattering and refraction, responsible for pulse energy loss. The process of energy loss involving absorption, reflection, and scattering is referred to as attenuation, which increases with depth and frequency. Because a higher frequency of ultrasound results in increased absorption, the consequence is a decrease in the depth of visualization.
The nature of the speckle pattern can be categorized into one of three classes according to the number of scatterers per resolution cell or the so called scatterer number density (**SND**), spatial distribution and the characteristics of the imaging system itself. These classes are described as follows:
1. **FFS** (Fully formed speckle) pattern, which occurs when many fine randomly distributed scattering sites exist within the resolution cell of the pulse-echo system.

In this case, the amplitude of the backscattered signal can be modeled as a Rayleigh distributed random variable with a constant SNR of 1.92. Under such conditions, the textural features of the speckle pattern represent a multivariate signature of the imaging instrument and its point spread function. Blood cells are typical examples of this type of scatterers.
2. Non randomly distributed with long-range order (**NRLR**). Examples of this type are the lobules in liver parenchyma. It contributes a coherent or specular backscattered intensity that is in itself spatially varying. Due to the correlation between scatterers, the effective number of scatterers is finite. This situation can be modeled by the K-distribution. This type is associated with SNR below 1.92. It can also be modeled by the Nakagami distribution.

3. Non randomly distributed with short-range order (**NRSR**). Examples of this type include organ surfaces and blood vessels. When a spatially invariant coherent structure is present within the random scatterer region, the probability density function (**PDF**) of the backscattered signals becomes close to the Rician distribution. This class is associated with SNR above 1.92 [10]

4.4 Need for despeckling:

Image quality is important when evaluating ultrasound images for the assessment of the degree of diseases, or when transferring images through a telemedicine channel, and/or in other image processing tasks and it effect by speckle noise. Thus, speckle is considered as the dominant source of noise in ultrasound imaging and should be processed without affecting important image features.[10]

The main purposes for speckle reduction in medical ultrasound imaging are:

1. To improve the human interpretation of ultrasound image–speckle reduction makes an ultrasound image cleaner with clearer boundaries.

2. Despeckling is a preprocess step for many ultrasound image processing tasks such as segmentation and registration –speckle reduction improves the speed and accuracy of automatic and semiautomatic segmentation and registration.[10]

4.5 Speckle reduction methods

Several techniques have been proposed for despeckling in medical ultrasound imaging. In this section we present the classification and theoretical overview of existing despeckling techniques:[12]

4.5.1. Compounding Methods

In this method a series of ultrasound images of the same target are acquired from different scan directions and with different transducer frequencies or under different strains. Then the images are averaged to form a composite image. The compounding method can improve the target detectability but they suffer from degrade spatial resolution and increased system complexity.[13]

4.5.2. Post-Acquisition Methods

This method do not require many hardware modification .The post-acquisition image processing technique falls under two categories

(1)Single scale spatial filtering (2) Multi scale Methods.[13]

4.5.2.1. Single scale spatial filtering Methods

A speckle reduction filter that changes the amount of smoothing according to the ratio of local variance to local mean was developed .in that method smoothing is increased in homogeneous region where speckle is fully developed and reduced or even avoided in other regions to preserve details.[13]

An unsharp masking filter was suggested in which the smoothing level is adjusted depending on the statistics of log compressed images. The above mentioned filters have difficulty in removing speckle near or on image edges. [13]

-Recently proposed filter utilizing short line segments in different angular orientations and selecting the orientation that is most likely to represent a line in the image .This technique poses a trade-off between effective line enhancement and speckle reduction. [13]

-Numbers of Region growing based spatial filtering methods have been proposed. In these methods it is assumed that pixels that have similar gray level and connectivity are related and likely to belong to the same object or region. After all pixels are allocated to different groups, spatial filtering is performed based on the local statistics of adaptive regions whose sizes and shapes are determined by the information content of the image .The main difficulty in applying region growing based methods is how to design appropriate similarity criteria for region growing. Different types of filters are used in the application of despeckling in ultrasound imaging. The most commonly used types of filters are: [13]

A. **Mean Filter -** has the property of locally reducing the variance thus reducing SNR and it requires the user to specify only the size of the window. However it has the effect of potentially blurring the image. This filter is optimal for additive Gaussian noise whereas the speckled image obeys a multiplicative model with non-Gaussian noise. Therefore simple mean is not the optimal choice. [14]

B. **Median Filters** are utilized for despeckling due to their robustness against impulsive type noise and edge preserving characteristics. The median filter produces less blurred images. The compounding procedure uses both the mean and median filters. [14]

4.5.2.2. Multi scale Methods:

Several multi scale methods based on wavelet and pyramid have been proposed for speckle reduction in ultrasound imaging. It classified to: [13]

4.5.2.2.1. Wavelet based speckle reduction methods.

The wavelet based speckle reduction method usually include

(1) Logarithmic transformation.

(2) Wavelet transformation.

(3) Modification of noisy co efficient using shrinkage function.

(4) Invert wavelet transform.

(5) Exponential transformation. This method can be classified into three groups:

1. **Thresholding methods -** The wavelet coefficients smaller than the predefined threshold are regarded as contributed by noise and then removed. The thresholding techniques have difficulty in determining an appropriate threshold.[11]

2. **Bayesian estimation methods –** This Method approximates the noise free signal based on the distribution model of noise free signal and that of noise. Thus, reasonable distribution models are crucial to the successful application of these techniques to medical ultrasound imaging.[11]

3. **Coefficients correlation methods -** This is an un decimated or over complete wavelet domain denoising method which utilizes the correlation of useful wavelet coefficients across scales. However this method does not rely on the exact prior knowledge of the noise distribution and this method is more flexible and robust compared to other wavelet based methods. [11]

4.5.2.2.2. Pyramid based speckle reduction methods

Pyramid transform has also been used for reducing speckle. Approximation and interpolation filters in pyramid transform have low pass properties so that pyramid transform does not require quadrature mirror filters unlike sub band decomposition in wavelet transform. [11]

A ratio Laplacian pyramid was introduced by considering the multiplicative nature of speckle. This method extended the conventional Kaun filter to multi scale domain by processing the interscale layers of the ratio Laplacian pyramid. But this method differs from the need to estimate the noise variance in each interscale layers.

A speckle reduction method based on non linear diffusion filtering of band pass ultrasound images in the Laplacian pyramid domain has been proposed which effectively suppresses the speckle while preserving edges and detailed features.[11]

4.6. Speckle Noise Modeling

To be able to derive an efficient despeckle filter, a speckle noise model is needed. The speckle noise model for ultrasound images may be approximated as multiplicative. The signal at the output of the receiver demodulation module of the ultrasound imaging system may be defined as

$$Y_{i,j} = x_{i,j} n_{i,j} + a_{i,j} \qquad (4.1)$$

where $Y_{i,j}$represents the noisy pixel in the middle of the moving window, $x_{i,j}$represents the noise free pixel, $n_{i,j}$ and $a_{i,j}$ represent the multiplicative and additive noise, respectively, and i, j are the indices of the spatial locations that belong in the 2D space of real numbers, i, j ϵ R2. [12]

Despeckling is based on estimating the true intensity $x_{i,j}$as a function of the intensity of the pixel $Y_{i,j}$and some local statistics calculated on a neighborhood of this pixel. [12]

the histogram of amplitudes within the resolution cells of the envelope-detected RF signal backscattered from a uniform area with a sufficiently high scatter density has a Rayleigh distribution with mean proportional to the standard deviation s (with $\mathrm{m}/\mathrm{s} = 1.91$). This implies that speckle could be modeled as multiplicative noise. [12]

However, the signal processing stages inside the scanner modify the statistics of the original signal, i.e., the logarithmic compression. The logarithmic compression is used to adjust the large echo dynamic range (50–70 dB) to the number of bits (usually 8) of the digitization module in the scan converter. More specifically, logarithmic compression affects the high-intensity tail of the Rayleigh and Rician probability density functions more than the low-intensity part. As a result, the speckle noise becomes very close to the white Gaussian noise corresponding to the uncompressed Rayleigh signal. In particular, it should be noted that speckle is no longer multiplicative in the sense that, on homogeneous regions, where x $_{i,}$j can be assumed constant, the mean is proportional to the variance (m » s 2) rather than the standard deviation (m » s). In this respect, the speckle index C will be for the log-compressed ultrasound images, i.e., $\mathrm{C} = \mathrm{s}\ 2/\mathrm{m}$.

Referring back to Eq. (4.1), since the effect of the additive noise is considerably smaller compared with that of the multiplicative noise, it may be written as

$$Y_{i,j} \gg x_{i,j} n_{i,j} \tag{4.2}$$

Thus, the logarithmic compression transforms the model in Eq. (4.2) into the classical signal in the additive noise form as

$$\log Y_{i,j} = \log x_{i,j} + \log n_{i,j} \tag{4.3}$$

and

$$g_{i,j} = f_{i,j} + n_{i,j} \tag{4.4}$$

The term $\log(Y_{i,j})$which is the observed pixel on the ultrasound image display after logarithmic compression, is denoted as $g_{i,j}$, and the terms $\log(x_{i,j})$ and $\log(n_{i,j})$, which are the noise-free pixel and the noise component after logarithmic compression, are denoted as $f_{i,j}$and $n_{i,j}$, respectively [see Eq. (4.4)].[12]

4.7. Despeckling filter

In this section several despeckling techniques such as Median, hybrid median filter, geometric filtering, linear scaling filter, Anisotropic diffusion filtering, speckle reducing Anisotropic diffusion filtering, wavelet filter are discussed.[15]

4.7.1. Nonlinear filtering

Non linear filtering is based on non linear operation involving the pixels in a neighborhood .for example, letting the center pixel in the moving window be equal to the maximum pixel in its neighborhood is anon linear filtering operation.[16]

4.7.1.1Median Filter

It is a spatial domain filter. A median filter generally smoothens the image to reduce noise and at the same time it preserves edges. It replaces the middle pixel in the window with the median-value of its neighbors. This filter does not create new pixel value. Instead it chooses the median value which is selected from the neighborhood. This will not affect other pixels significantly. Hence this filter preserves the edges; this filter is relatively slow, even with fast sorting algorithms such as quick sort. The median filter does not blur the contour of the objects. [16]

4.7.1.2Hybrid Median Filter

The hybrid median filter is another modification of median filter. This filter is also called as corner preserving median filter is a three-step ranking operation. In a 5X5 pixel neighborhood, pixels can be ranked in two different groups as shown in fig.4.2.

The median values of the 45^o neighbors forming an "X" and the 90^o neighbors forming a "+" are compared with the central pixel and the median value of that set is then saved as the new pixel value.

The three step ranking operation does not impose a serious computational penalty as in the case of median filter. Each of the ranking operations is for a much smaller number of values than used in a square region of the same size. For example, the 5 pixel wide neighborhood used in the examples contains either 25 (in the square neighborhood) which must be ranked in the traditional method. In the hybrid method, each of the two groups contains only 9 pixels, and the final comparison involves only three values. Even with the additional logic and manipulation of values, the hybrid method is faster than the conventional median. This median filter overcomes the tendency of median and truncated median filters to erase lines which are narrower than the half width of the neighborhood and to round corners. [16]

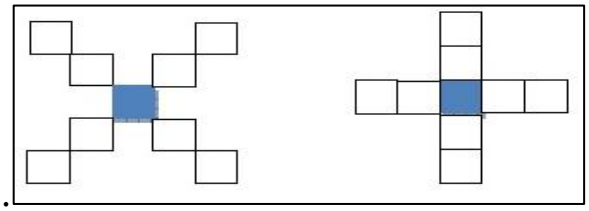

Figure 4.2.Diagram of neighborhood pixels used in the Hybrid median filter.[16]

4.7.1.3 Geometric Filtering

The concept of the geometric filtering is that speckle appears in the image as narrow walls and valleys. The geometric filter, through iterative repetition, gradually tears down the narrow walls (**bright edges**) and fills up the narrow valleys (**dark edges**), thus smearing the weak edges that need to be preserved.

The geometric filtering uses a nonlinear noise reduction technique. It compares the intensity of the central pixel in a 3 × 3 neighborhood with those of its eight neighbors and, based upon the neighborhood pixel intensities, it increments or decrements the intensity of the central pixel such that it becomes more representative of its surroundings.

Can see that although the result obtained by geometric filter, given poor performance for removing the speckle noise, it is lead to increasing the contrast significantly of the image. [17]

4.7.1.4 Linear Scaling Filter (DsFca, DsFls)

The linear scaling gray level (**DsFca**) filters despeckle the image through linear scaling of the gray-level values. In a window of [5*5] pixels, compute the mean of

all pixels whose difference in the gray level with the intensity $g_{i,j}$ (the middle pixel in the moving window) is lower than or equal to a given threshold ϑ. Assign this value to the gray level $g_{i,j}$ with $\vartheta = \alpha * g_{max}$, where g_{max} is the maximum gray level of the image and α = [0,1] , Best results can be obtained with α = 0,1.

The linear scaling (**DsFls**) has high degree of blurring and was effect on gray level because In a window of [5*5] pixels it is compute the mean of all pixels how's difference in the gray level with the intensity (the middle pixel in the moving window) is lower than or equal to a given threshold.[12]

4.7.1.5 Speckle Reducing Anisotropic Diffusion (SRAD)

Anisotropic Diffusion is a nonlinear smoothing filter which uses a variable conductance term that controls the contrast of the edges that influence the diffusion. This filter has the ability to preserve edges, while smoothing the rest of the image to reduce noise. The anisotropic diffusion has been used by several researchers in image restoration and image recovery.

SRAD is an edge-sensitive Partial Differential Equation (PDE) anisotropic diffusion approach to reduce speckle noise in images.

The anisotropic filtering in SRAD simplifies image features to improve image segmentation and smoothes the image in homogeneous area

While preserving edges and enhances them. It reduces blocking artifacts by deleting small edges amplified by homomorphic filtering.

SRAD equation for an image u is given by the Equation. [3]

$$SRAD(u`) = ut + 1 + ut + \left(\Delta t/_4\right) div(g\big(ICOV(u`)\big)x\Delta u` \tag{4.5}$$

Where, t is the diffusion time index, $f`t$ is the time step responsible for the convergence rate of the diffusion process (Normally in the range 0.05 to 0.25), g(.) is the diffusion Δ function and is given by equations :- [3]

$$G\big(ICOV(u`)\big) = e^{-(p)} \tag{4.6}$$

$$p = \frac{\left[\frac{ICOV(u`)}{q^t}\right]^2}{1+(\mathrm{qt})^2} \tag{4.7}$$

4.7.1.6 Wavelet filtering

The wavelet techniques are widely used in the image processing, such as the image compression, image de-noising. It has been shown that its performance of image processing is better than the methods based on other linear transformation.

The wavelet de-noising method decomposes the image into the wavelet basis and shrinks the wavelet coefficients in order to despeckle the image. From the noisy image, global soft threshold coefficients are calculated for every decomposition level. After the thresholding, the image is reconstructed by inverse wavelet transforming and the despeckled image is derived. After the wavelet transformation, the signal energy will only concentrate on several wavelet coefficients and the majority of the coefficients will become zeros. Also the frequency domain filtering based on the DFT could not work well to the piecewise smooth functions. It has been proved that the simple wavelet de-noising methods could provide almost optimal request to the polynomial piecewise signals.The errors of the estimation. [15]

$$E\ [\|x - x\|]^{2/N}\ is\ the\ same\ order\ O\ (\log 2^{N/N}) \qquad (4.8)$$

4.8 Limitation of despeckle filtering techniques

Despeckling is always a tradeoff between noise suppression and loss of information, which is something that experts are very concerned about. It is, therefore, desirable to keep as much important information as possible. The majority of speckle reduction techniques have certain limitations that can be briefly summarized as follows.

They are sensitive to the size and the shape of the window. The use of different window sizes greatly affects the quality of the processed images. If the window is too large, over smoothing will occur, subtle details of the image will be lost in the filtering process, and edges will be blurred.

On the other hand, a small window will decrease the smoothing capability of the filter and will not reduce the speckle noise, thus making the filter not effective.In homogenous areas, the larger the window size, the more efficient the filter in reducing the speckle noise. In heterogeneous areas, the smaller the window size, the more it is possible to keep subtle image details unchanged. Our experiments showed that a [3*3] window size is a fairly good choice.

Some of the despeckle methods based on window approaches require thresholds to be used in the filtering process, which have to be empirically estimated. There are a number of thresholds introduced in the literature, which include gradient thresholding, soft or hard thresholds, nonlinear thresholds, and wavelet thresholds. The inappropriate choice of a threshold may lead to average filtering and noisy boundaries, thus leaving the sharp features unfiltered.[17]

4.9Image Quality Evaluation Metrics

4.9.1 Pixel Difference Measurement

Objective evaluation of the image quality on ultrasound images is a comprehensive task due to the relatively low image quality compared to other imaging techniques. It is desirable to objectively determine the quality of ultrasound images since

quantification of the quality removes the subjective evaluation which can lead to varying results.
Differences between the original, $g_{i,}$, and the despeckled $f_{i,j}$, images were evaluated using image quality evaluation metrics.

The root mean square error (**RMSE**), which is the square root of the squared error averaged over an MxN window:

$$\text{RMSE}=\sqrt{\frac{1}{\text{MN}}\sum_{\text{i=1}}^{\text{M}}\sum_{\text{j=1}}^{\text{N}}\left(g_{i,j}-f_{i,j}\right)^2}. \tag{4.10}$$

The signal-to-noise ratio (**SNR**) is given by:

$$\text{SNR}= 10\log_{10}\frac{\sum_{\text{i=1}}^{\text{M}}\sum_{\text{j=1}}^{\text{N}}\left(g_{i,j}{}^2+f_{i,j}{}^2\right)}{\sum_{\text{i=1}}^{\text{M}}\sum_{\text{j=1}}^{\text{N}}\left(g_{i,j}-f_{i,j}\right)^2} \tag{4.11}$$

The peak SNR (**PSNR**) is computed using:

$$\text{PSNR}=10\log_{10}\frac{\text{MSE}}{g_{\text{max}}^2} \tag{4.12}$$

Where g_{max}^2 is the maximum intensity in the unfiltered image.
The PSNR is higher for a better-transformed image and lower for a poorly transformed image. It measures image fidelity, which is how closely the despeckled image resembles the original image. [12]

4.9.2 Human Visual Based Measurement

The HVS is a method that uses human eye as a reference. The main idea is that humans are interested in different attributes of the image other than taking it as a whole. These attributes include brightness, contrast, texture, orientation...etc. [18]

4.9.2.1 Universal Image Quality Index (UIQI)

Universal Image Quality, it breaks the comparison between original and distorted image into three comparisons: luminance, contrast, and structural comparisons.[18]

$$I(x,y)=\frac{2\mu x\mu y}{\mu_x^2+\mu_y^2} \tag{4.13}$$

$$C(x,y)=\frac{2\sigma_x\sigma_y}{\sigma_x^2+\sigma_y^2} \tag{4.14}$$

$$S(x,y) = \frac{2\sigma xy}{\sigma_x \sigma_y} \quad (4.15)$$

Where $\mu x \mu y$ denotes the mean values of original and $\sigma_x \sigma_y$ distorted images. And σ_{xy} denotes the standard deviation of original and distorted images, and is the covariance of both images.

Based on the above three comparisons the UIQI is given as:

$$UIQI(x,y) = I(x,y).C(x,y).S(x,y) = \frac{4\mu_x \mu_y \mu_{xy}}{(\mu_x^2+\mu_y^2)(\sigma_x^2+\sigma_y^2)} \quad (4.16)$$

UIQI is a simple measure that counts only on first and second order statistic of the original and distorted images.[18]

4.9.2.2 Structural Similarity Index (SSIM):

The structural similarity index an improvement for UIQI, SSIM between two images is given by:

$$\text{SSIM}=\frac{(2\bar{gf}+c_1)(2\sigma_{gf}+c_2)}{(\bar{g}^2+\bar{f}^2+c_1)(\sigma_g{}^2+\sigma_f{}^2+c_2)}, \ -1<\text{SSIM}<1, \quad (4.17)$$

Where c_1 = 0.01dr and c_2 = 0.03dr, with dr = 255 representing the dynamic range of the ultrasound images. The range of values for the SSIN lies between −1, for a bad and 1 for a good similarity between the original and despeckled images, respectively. It is computed, for a sliding window of size 8 × 8 without overlapping. [18]

4.9.2.3 Edge Preservation Factor (EPF)

The edge preservation ability of the filter is compared by Edge Preservation Factor and is computed using:

$$EPF = \frac{\sum(\Delta x-\overline{\Delta x})(\Delta y-\overline{\Delta y})}{\sqrt{\sum(\Delta x-\overline{\Delta x})^2 \sum(\Delta y-\overline{\Delta y})^2}} \quad (4.18)$$

Where Δx and Δy are the high pass filtered versions of images x and y, obtained with a 3x3 pixel standard approximation of the Laplacian operator. The larger value of EPF means more ability to preserve edges. [19]

To quantify the performance improvements of the speckle reduction method and edges detection operators various measures may be used. The commonly preferred measures are root mean squared error (RMSE), signal to noise ratio (SNR), peak signal to noise ratio(PSNR), Universal Image Quality Index(UIQI), structural

similarity index(SSIM) and Edge Preserving Factor(EPF) 'which specially for edges assessment' which have been calculated from the denoised US images and are found in the literatures. The PSNR and SNR is higher for a better-transformed image and lower for a poorly transformed image, on the contrary in RMSE. Whilst the range of values for the UIQI ,SSIM and EPF lies between -1, for bad and 1 for good similarity between the original and despeckled images.

4.10 Edge Model Definition

An edge corresponds to local intensity discontinuities of an image. In the real world, the discontinuities reflect a rapid intensity change, such as the boundary between different regions, shadow boundaries, and abrupt changes in surface orientation and material properties. For example, edges represent the outline of a shape, the difference between the colors and pattern or texture. Therefore, edges can be used for boundary estimation and segmentation in scene understanding. They can also be used to find corresponding points in multiple images of the same scene. For instance, the fingerprint, human facial appearance and the body shape of an object are defined by edges in images. In a broad sense the term edge detection refers to the detection and localization of intensity discontinuities of these image properties. In a more restrictive sense, it only refers to locations of significant change of intensity. Points of these locations are called edges or edge elements. Figure 4.3 shows images in which edges define object size, shape, scene and human appearance.[20]

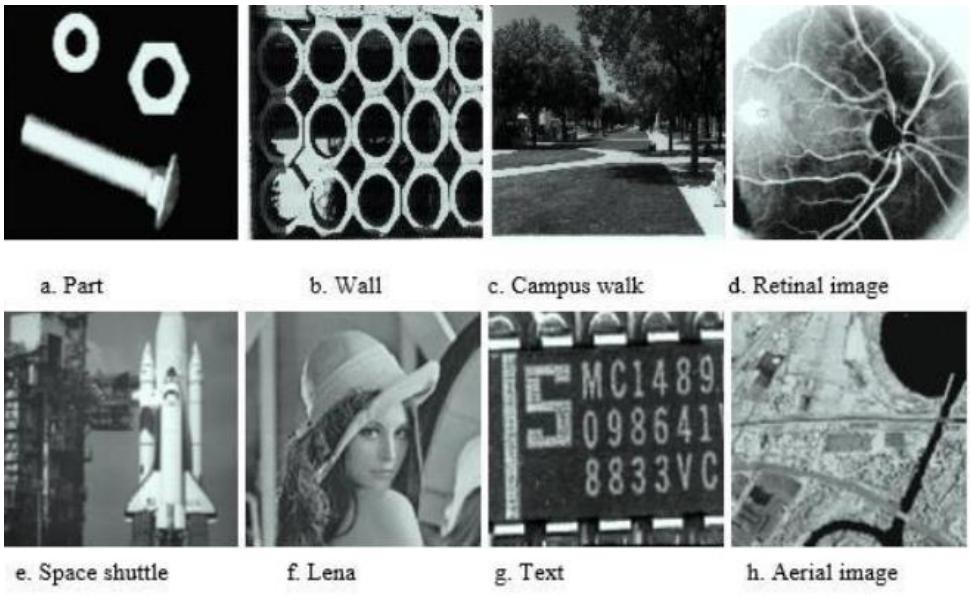

Figure 4.3: Edges in image show object size, shape, boundary, human facial appearance [20]

The difference between boundaries and edges is that boundaries are the linked edges that characterize the shape of an object. Edges are piecewise segmentation. They are both useful in computation of geometrical features such as shape or orientation. Edge detection is grounded on the assumption that physical 3-dimensional shapes in the scene, such as object boundaries and shadow boundaries, are clues for the characterization of the scene.[20]

4.11 Effects of noise on edge detection

Edge detection is susceptible to noise. This is due to the fact that the edge detectors algorithms are designed to respond to sharp changes, which can be caused by noisy pixels. Noise may occur in digital images for a number of reasons. The most commonly studied noises are white noise. To reduce the effects of noise, preprocessing of the image is performed. The preprocessing can be performed in two ways, filtering the image with a Gaussian function, or by using a smoothing function. The problem with the above approaches is that the optimal result may not be obtained by using a fixed operator.[21]

4.12 Why Do We Need Edge Detection?

In general, edge detection is the process that attempts to characterize the intensity changes in terms of the physical processes that have originated them. Edge detection can be used for region segmentation, feature extraction and object or boundary description. Edges provide the topology and structure information of objects in an image. For example, different cars can be easily recognized from their body shape. The highway and river from aerial images can be detected in terms of their structure or distribution pattern, which all are described by edges. By using edge detection techniques, machine vision and image processing systems can be built for a variety of applications. For example, edge detection can be used in assembly line inspection to detect defects of mechanical parts and in semiconductor manufactory. Edge detection can be used for locating the road and recognizing obstacles in automatic vehicle navigation. Edge detection also can be used to detect military targets in remote sensor applications. For medical imaging applications, edge detection and boundary segmentation can be used for locating tumors and blood vessels, and rigid bony structures. Edge detection, therefore, is consistent with human visual response, which will provide edge strength and orientation for feature extraction and object description. For reducing information being processed, after edge detection gray scale edges are usually converted into binary images by thresholding. The transformation preserves a great deal of the primitive or intrinsic information from the original image, i.e., the outline of the

shape. Later image processing can handle this simple form for recognition, matching or compression.[21]

4.13 Difficulty with the Process of Edge Detection

Edge detection is a difficult issue. One difficulty comes from the complex contents of image itself. In real world applications, images contain object boundaries and object shadows and noise. The second cause of problems is degradation in image acquisition. Sometimes it may be difficult to distinguish the exact edge from noise or trivial geometric features. Two level edge detection processes are often used since the difficulty of edge estimation cannot be easily overcome from detection operators alone. The first level process, called low-level process, extracts pieces of raw edge segments and geometric features, called primitives. They may be incomplete and inaccurate. The second level process usually is called high-level process. It will interpret and combine raw edges based on the edge models or deduction rules from a broader image context and a knowledge database. Sometimes pattern matching and statistical analysis will occur at this level. The second level process tries to remove the uncertainty or make correct decisions using low-level inputs and context. The more accurate the low-level input is, the more accurate the high-level process result will be achieved. To measure the quality of low-level process, several criteria are proposed to help to improve the accuracy of edge detection.[21]

4.14 Criteria for Edge Detection

The quality of edge detection can be measured from several criteria objectively. Some criteria are proposed in terms of mathematical measurement, some of them are based on application and implementation requirements. In all cases a quantitative evaluation of performance requires use of images where the true edges are known. [22]

Good detection: There should be a minimum number of false edges or maximum Signal Noise Ratio (SNR). Usually, edges are detected after a threshold operation. The high threshold will lead to less false edges, but it also reduces the number of true edges detected..

Noise sensitivity: The robust algorithm can detect edges in certain acceptable noise (Gaussian, Uniform and impulsive noise) environments. Actually, an edge detector the edges and also amplifies the noise simultaneously. Strategic filtering, consistency checking and post processing (such as non-maximum suppression) can be used to reduce noise sensitivity [23].

Good localization: The edge location must be reported as close as possible to the correct position, i.e. edge localization accuracy [23][24].

Orientation sensitivity: The operator not only detects edge magnitude, but it also detects edge orientation correctly. Orientation can be used in post processing to connect edge segments, reject noise and suppress non-maximum edge magnitude.

Speed and efficiency: The algorithm should be fast enough to be usable in an image processing system. An algorithm that allows recursive implementation or parable processing can greatly improve efficiency.

Criteria of edge detection will help to evaluate the performance of edge detectors. Correspondingly, numerous techniques have been developed to achieve the targets listed above in terms of local region process, which can be classified into linear and nonlinear techniques.[24]

4.15 Edge Detection Techniques

4.15.1 Robert's cross Operator

The Roberts Cross operator performs a simple, quick to compute, 2-D spatial gradient measurement on an image. Pixel values at each point in the output represent the estimated absolute magnitude of the spatial gradient of the input image at that point.

The operator consists of a pair of 2×2 convolution kernels as shown in Figure. One kernel is simply the other rotated by 90°. This is very similar to the Sobel operator.

Figure 4.4: Roberts operator [25]

These kernels are designed to respond maximally to edges running at 45° to the pixel grid, one kernel for each of the two perpendicular orientations. The kernels can be applied separately to the input image, to produce separate measurements of the gradient component in each orientation (call these *Gx*

and *Gy*). These can then be combined together to find the absolute magnitude of the gradient at each point and the orientation of that gradient. The gradient magnitude is given by:

$$|G| = \sqrt{Gx^2+Gy^2} \tag{4.19}$$

Although typically, an approximate magnitude is computed using:

$$|G| = |G_x| + |G_y| \tag{4.20}$$

which is much faster to compute[25]. The angle of orientation of the edge giving rise to the spatial gradient (relative to the pixel grid orientation) is given by:

$$\theta = \arctan(Gx/Gy) - \tfrac{3\pi}{4} \tag{4.21}$$

4.15.2 Prewitt's Operator

The Prewitt edge detection is proposed by Prewitt. To estimate the magnitude and orientation of an edge Prewitt is a correct way. Even though different gradient edge detection wants a quiet time consuming calculation to estimate the direction from the magnitudes in the x and y-directions, the compass edge detection obtains the direction directly from the kernel with the highest response. It is limited to 8 possible directions; however knowledge shows that most direct direction estimates are not much more perfect. This gradient based edge detector is estimated in the 3x3 neighborhood for eight directions. All the eight convolution masks are calculated. One complication mask is then selected, namely with the purpose of the largest module.

-1	-1	-1
0	0	0
+1	+1	+1

G_x

-1	0	+1
-1	0	+1
-1	0	+1

G_y

Figure 4.5: Prewitt's operator [26]

Prewitt detection is slightly simpler to implement computationally than the Sobel detection, but it tends to produce somewhat noisier results [26].

4.15.3 Laplacian of Gaussian (LoG)

The Laplacian is a 2-D isotropic measure of the 2nd spatial derivative of an image. The Laplacian of an image highlights regions of rapid intensity change and is therefore often used for edge detection. The Laplacian is often applied to an image that has first been smoothed with something approximating a Gaussian Smoothing.

0	-1	0
-1	4	-1
0	-1	0

G_x

-1	-1	-1
-1	8	-1
-1	-1	-1

G_y

Figure 4.6: (LoG) operator [25]

Filter in order to reduce its sensitivity to noise. The operator normally takes a single gray level image as input and produces another gray level image as output [25]. The Laplacian $L_{(x,y)}$ of an image with pixel intensity values $I_{(x,y)}$ is given by:

$$L(x,y)_{=\frac{\partial^2 I}{\partial x^2}+\frac{\partial^2 I}{\partial y^2}} \tag{4.22}$$

Since the input image is represented as a set of discrete pixels, we have to find a discrete convolution kernel that can approximate the second derivatives in the definition of the Laplacian [25].The Laplacian is generally used to found whether a pixel is on the dark or light side of an edge [26].

4.15.4 Canny's Edge Detection

In industry, the canny edge detection technique is one of the standard edge detection techniques. It was first created by John Canny for his Master's thesis at MIT in 1983, and still outperforms many of the newer algorithms that have been developed. To find edges by separating noise from the image before find edges of image the Canny is a very important method. Canny method is a better method without disturbing the features of the edges in the image afterwards it applying the tendency to find the edges and the serious value for threshold [26]. The algorithmic steps are as follows:

- Convolve image $f(r,\ c)$ with a Gaussian function to get smooth image $f\hat{}(r,c)$.

$$f\hat{}(r,c) = f(r,c) * G(r,c,6) \quad (4.23)$$

- Apply first difference gradient operator to compute edge strength then edge magnitude and direction are obtain as before.
- Apply non-maximal or critical suppression to the gradient magnitude.
- Apply threshold to the non-maximal suppression image.

4.15.5 Sobel Operator

The operator consists of a pair of 3×3 convolution kernels as shown in Figure (4-7). One kernel is simply the other rotated by 90°.

-1	0	+1
-2	0	+2
-1	0	+1

Gx

+1	+2	+1
0	0	0
-1	-2	-1

Gy

Figure 4.7: Masks used by Sobel Operator [26]

These kernels are designed to respond maximally to edges running vertically and horizontally relative to the pixel grid, one kernel for each of the two perpendicular orientations. The kernels can be applied separately to the input image, to produce separate measurements of the gradient component in each orientation (call these Gx and Gy). These can then be combined together to find the absolute magnitude of the gradient at each pointand the orientation of that gradient [26]. The gradient magnitude is given by:

$$|G| = \sqrt{Gx^2+Gy^2} \quad (4.24)$$

Typically, an approximate magnitude is computed using:

$$|G| = |G_x| + \left|G_y\right| \quad (4.25)$$

Which is much faster to compute [26].

The angle of orientation of the edge (relative to the pixel grid) giving rise to the spatial gradient is given by:

$$\theta = \arctan(Gx/Gy) \tag{4.26}$$

4.15.6 Zero Crossing method:

The zero crossing detector looks for places in the Laplacian of an image where the value of the Laplacian passes through zero i.e. points where the Laplacian changes sign. Such points often occur at `edges' in images i.e. points where the intensity of the image changes rapidly, but they also occur at places that are not as easy to associate with edges. It is best to think of the zero crossing detector as some sort of feature detector rather than as a specific edge detector. Zero crossings always lie on closed contours, and so the output from the zero crossing detector is usually a binary image with single pixel thickness lines showing the positions of the zero crossing points.

The starting point for the zero crossing detector is an image which has been filtered using the Laplacian of Gaussian filter. The zero crossings that result are strongly influenced by the size of the Gaussian used for the smoothing stage of this operator. As the smoothing is increased then fewer and fewer zero crossing contours will be found, and those that do remain will correspond to features of larger and larger scale in the image.[27]

CHAPTER FIVE

Materials and Methodology

5.1 Introduction

The proposed method was developed using the MATLAB 2013 for the implementation of edge detection technique in medical image. This high performance language for technical computer, integrates computation, visualization, and programming in an easy-to-use environment. One of the reasons of selecting MATLAB in this thesis is because it fits perfectly in the requirements of an image processing research due to its inherent characteristics. Image Processing Toolbox of MATLAB provides a broad set of reference standard algorithms and graphical tools for image processing such as analysis, image enhancement, feature detection, noise reduction and image registration etc. Image processing toolbox supports a diverse set of image types, including high dynamic range, high resolution.

The images of US used in the implementation of the proposed method were download from the Children`s Hospital of Philadelphia database of **Fetal** ultrasound image, and IBE Tech (Giza. Egypt) database of ultrasound image including **Liver**. In this thesis a data set of US images were used. Then read and displayed the US images in the MATLAB software. These images processed prior to the application of the edge detection technique. The methodology consists of two essentially steps, *firstly*: the **pre-process** step. The first step in processing the noise addition and several types of despeckling filters effective in removal of this type of noise applied to remove the noise and build up the Modified Hybrid Median Filter (MHMF) which will be illustrates next part. Next, comparing the values of the RSME, SNR, PSNR and UIQI between proposed method MHMF and other despeckling filters in order to assess the filter performance. *Secondly:* in **Evaluation** step, find MHMF output image edge using number of well-known techniques to detect edges. And compare the SNR, PSNR,RSME,UIQI and EPF between MHMF and normal HMF. and after comparing the result and clarity of its effectiveness.

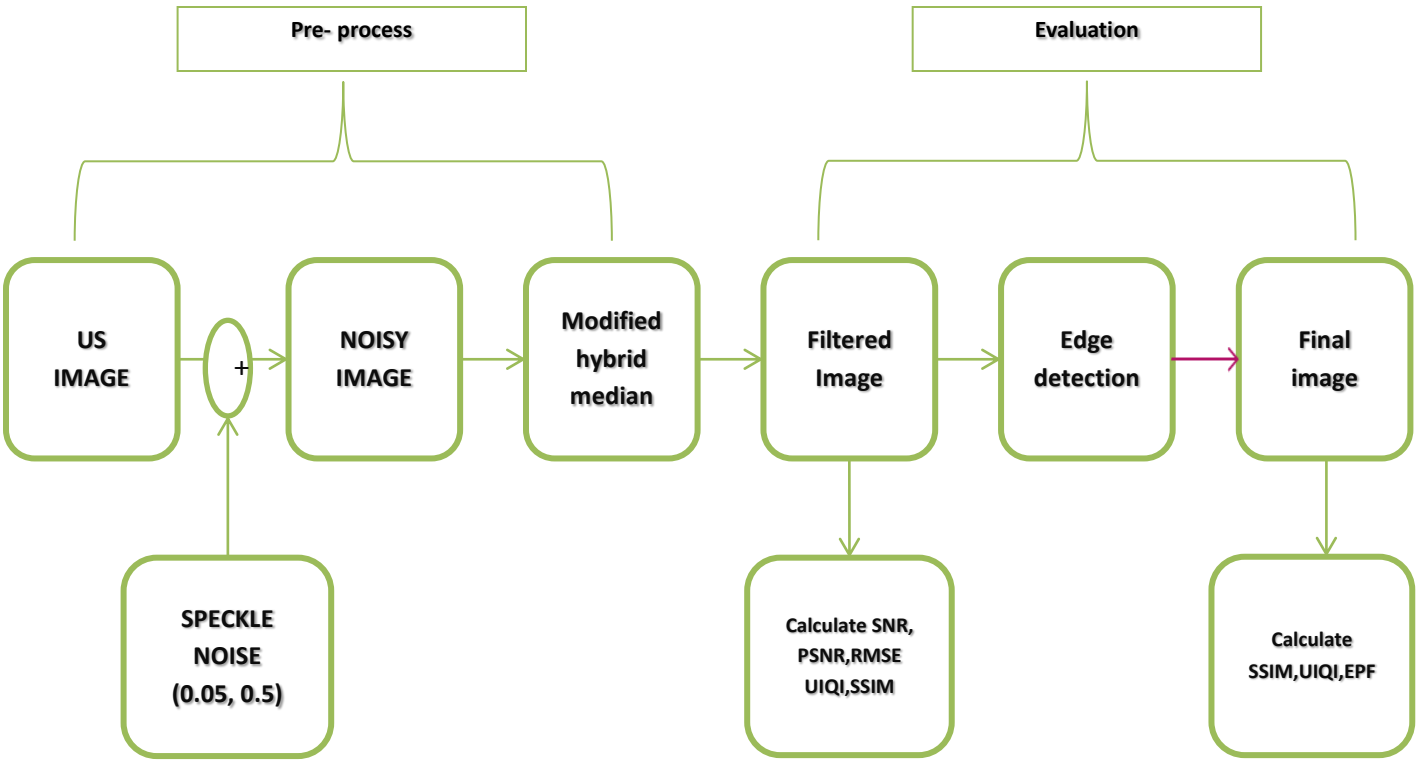

Figure 5.1: flow chart of proposed method

5.2 Noise addition and filtering

In this step the images are artificially corrupted by speckle noise (multiplication noise) with variance **σn** = 0.05 and 0.5 using the MATLAB command "imnoise (image, speckle‟, 0.05 or 0.5)”. Several types of filters such as linear scaling gray level filter(DsFca),geometric despeckle filter(DsFg), linear scaling(DsFls), speckle reducing anisotropic diffusion(srad), median filter(Med),hybrid median filter(HMF), wavelet filter have been implemented in the same US images with both variance value.

5.3 Edge detection technique

In this section six techniques were applied, detection operators were used (canny, sobel , prewitt , zero-cross, roberts and laplacian of guassian) It has been talk about them in detail in Chapter four. And compute image quality evaluation metrics to evaluated the result and chose best edge operator.

Figure 5.2 : Edge detection flow chart

5.4 Proposed Method: Modified Hybrid Median Filter (MHMF)

This proposed filter is the modified version of the hybrid median filter. It works on the sub windows similar to hybrid median filter. The **mean** and **median** values of the 45^o neighbours forming an **"X"** and the **maximum** value of 90^o neighbours forming a **"+"** as shown in Fig.1.are compared with the central pixel and the **median** value of that set are then saved as the new pixel value.

Figure. 5.3: The sub windows of proposed method (a) The median value of the 45^o neighbours. (b) The max value of the 90^o neighbours.

Algorithm:-

1. Find the maximum ***MXR*** of the pixels marked as **R** and the central pixel **C** in the 5x5 window

2. Find the median ***MD*** of the pixels marked as **D** and the central pixel C in the 5x5 window

3. Find the mean ***MND*** of the pixels marked as **D** and the central pixel C in the 5x5 window

3. Finally compute ***MM***.

MM = median (MXR, MD,MND)

4. Filter value $X_{i,j}$ =*MM*.

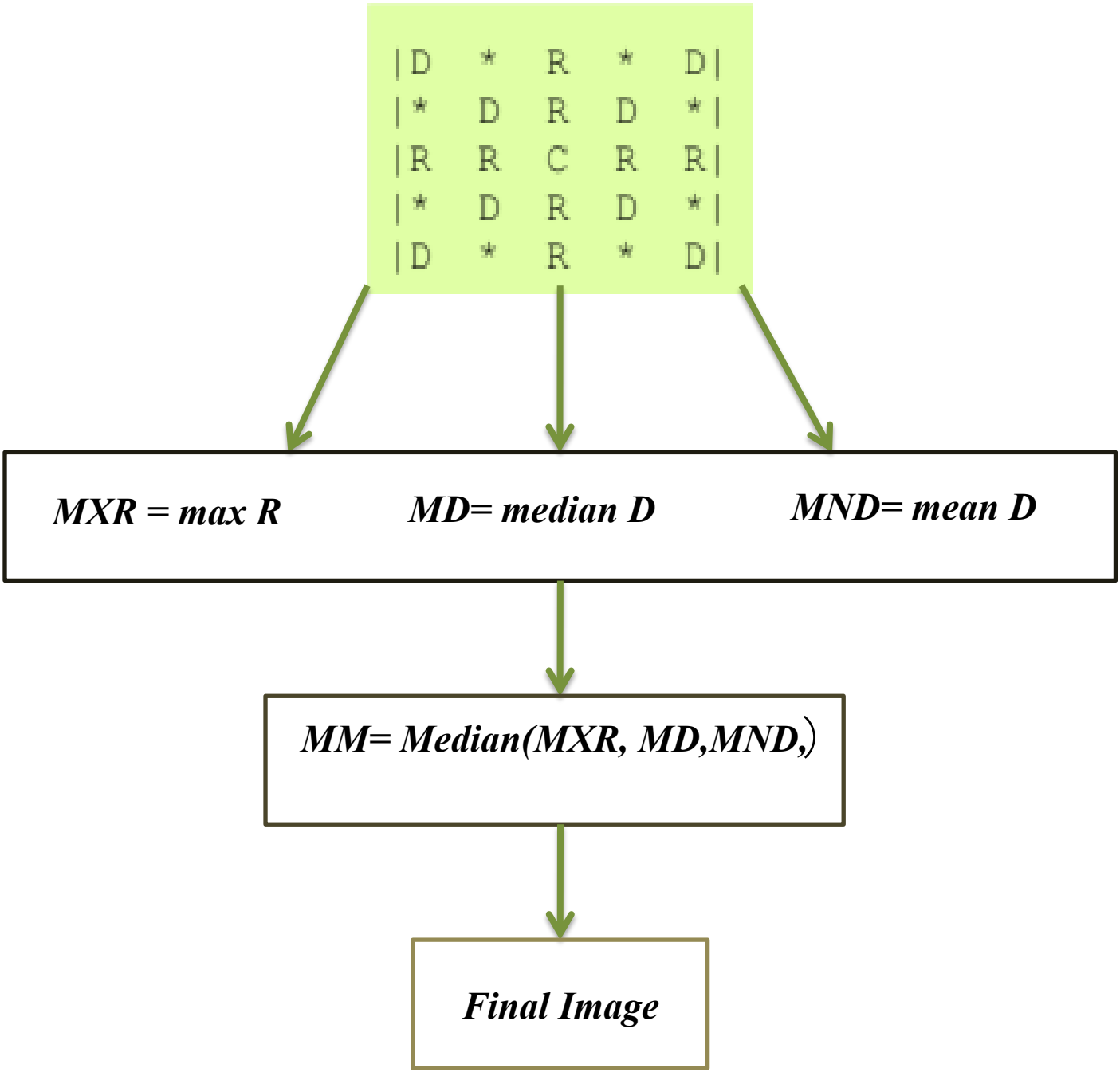

Figure 5.4: flow chart of modified Hybrid Median Filter

CHAPTER SIX

6.1 Experimental result

In this chapter, the differences between the original, and the despeckled images were evaluated using image quality evaluation metrics. The following measures, which are easy to compute and have clear physical meaning.

The test results of US B-scan images namely **Fetal**, **liver** with the two variance value of multiplication noise (**σn**= 0.5 and 0.05) given in figures 6.1, 6.3, 6.5, 6.7, 6.9 Also the performance image quality evaluation metrics calculated from the denoised image of the different filters are summarized in Tables from 6.1 to 6.4 for comparison.

Pre-process step:

(A) Original image

(B) Noisy image

(C) DsFca

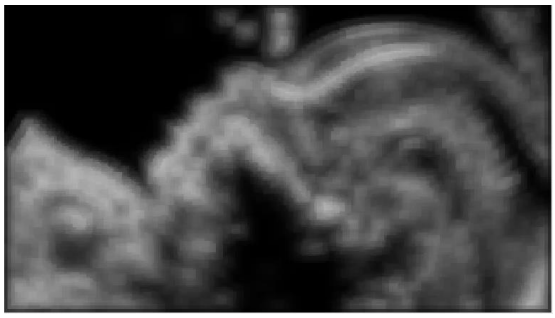

(D) DsFls

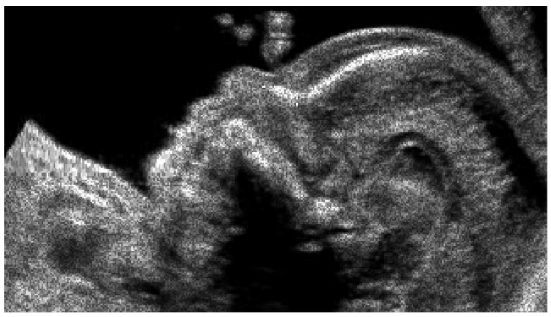

(E) DsFg

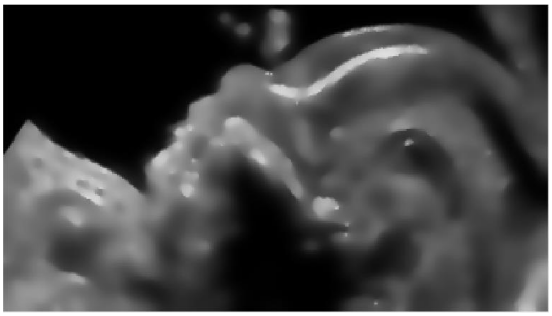

(F) SRAD

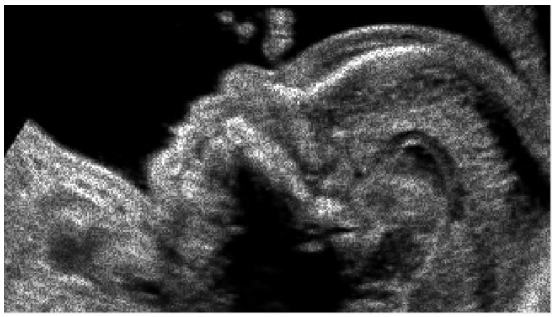

(G) Wavelet

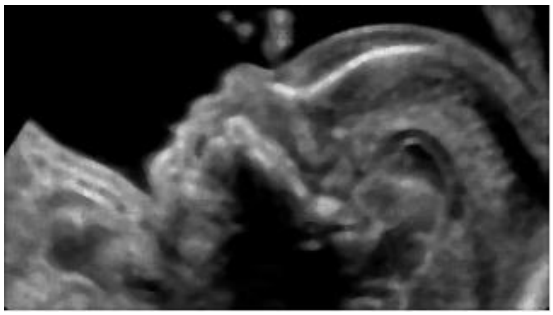

(H) Median

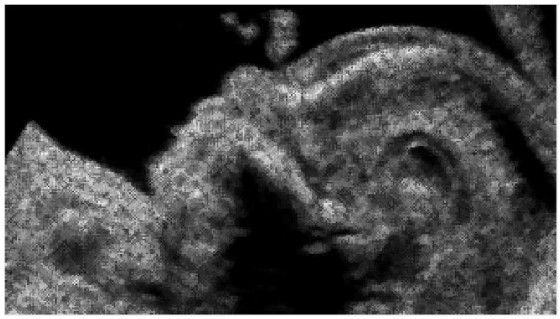

(I) HMF

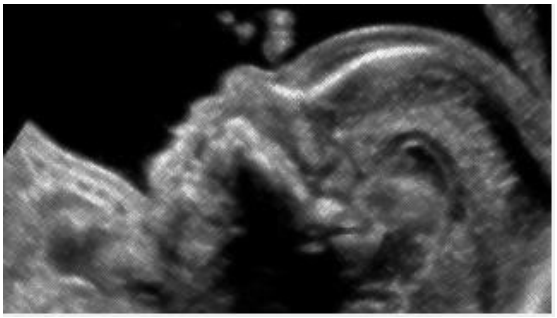

(J) Proposed Method

Figure 6.1 (A), (B), (C), (D), (E), (F), (G), (H), (I)and (J) original and noisy images and images filtered by DsFca, DsFls, DsFg, SRAD , Wavelet, Median, Hybrid Median Filter and proposed method Modified Hybrid Median Filter respectively Results of **Fetal** despeckled by mentioned filter on multiplication noise (**σn=0.05**)

Table 6.1: Image quality evaluation metrics computed for the **fetal** (σn=0.05) at statistical measurement of SNR ,RSME,PSNR,UIQI and SSIM for different filter types .

Filter	RMSE	SNR	PSNR	UIQI	SSIM
DsFls	24.0255	13.6951	23.5277	0.4540	0.5301
DsFca	17.4016	16.4968	26.3293	0.5672	0.6280
DsFg	14.9831	17.8107	27.6291	0.8045	0.7965
SRAD	20.7504	14.9172	24.8006	0.5177	0.6145
Wavelet	20.8230	14.9590	24.7702	0.7004	0.7315
Med	18.6384	15.7445	25.7329	0.7149	0.7623
HMF	32.3173	11.2891	20.9523	0.6553	0.7138
Proposed Method	**13.4597**	**18.9749**	**28.5604**	**0.8045**	**0.8277**

Bold number indicates the best values.

* signal-to-noise ratio (SNR), root mean square error (RSME) peak-to-noise ratio (PSNR), Universal Image Quality Index(UIQI), structural similarity index (SSIM).

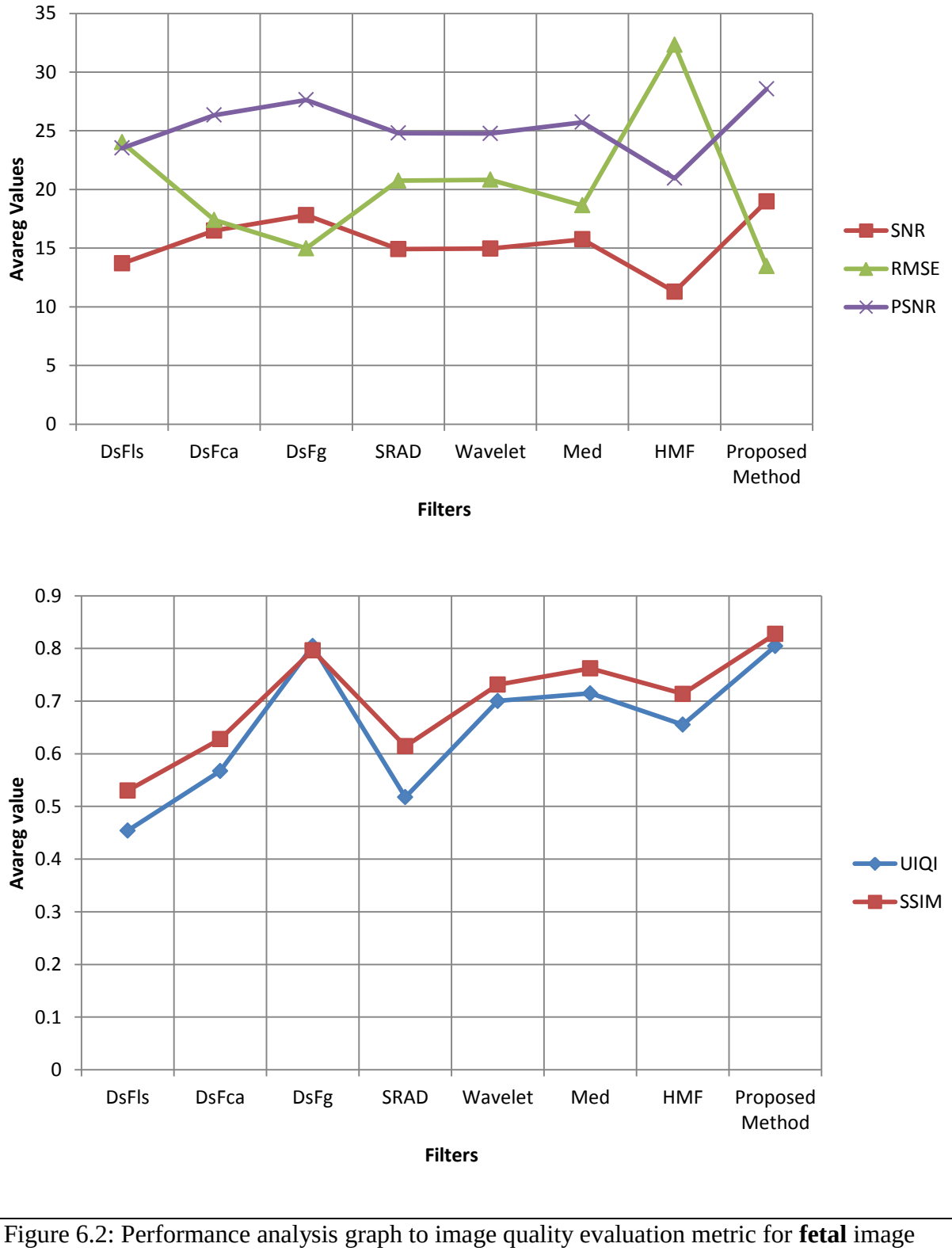

Figure 6.2: Performance analysis graph to image quality evaluation metric for **fetal** image

(noise **σn =0.05**)

(A) Original image

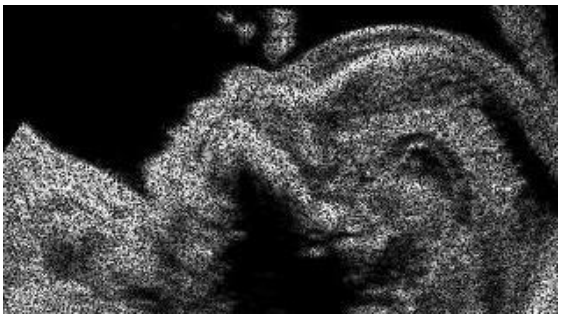

(B) Noisy image

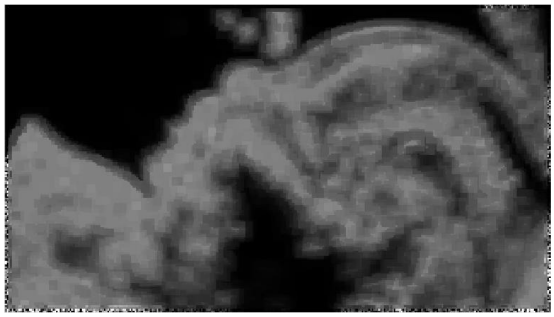

(C) DsFca

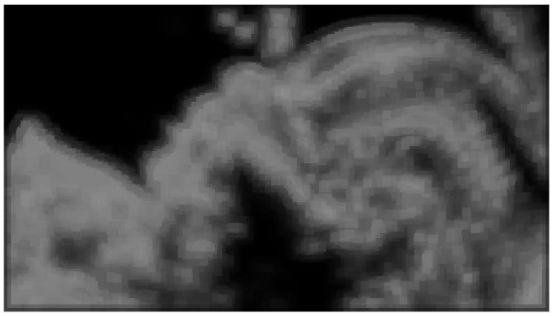

(D) DsFls

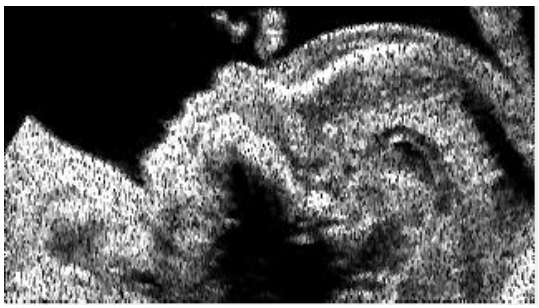

(E) DsFg

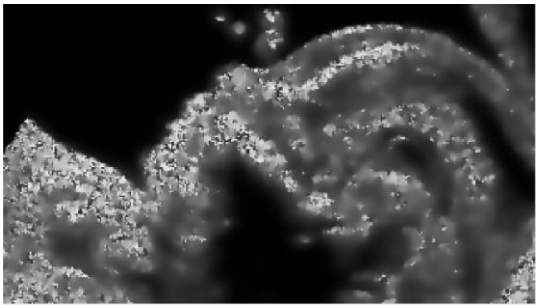

(F) SRAD

(G) Wavelet

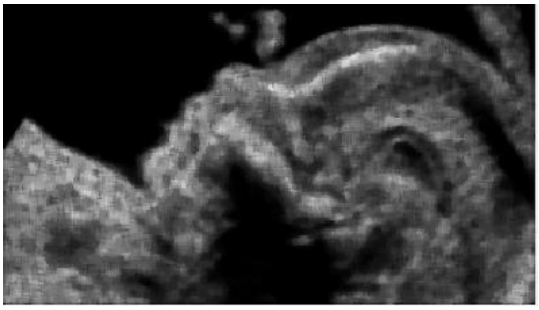

(H) Median

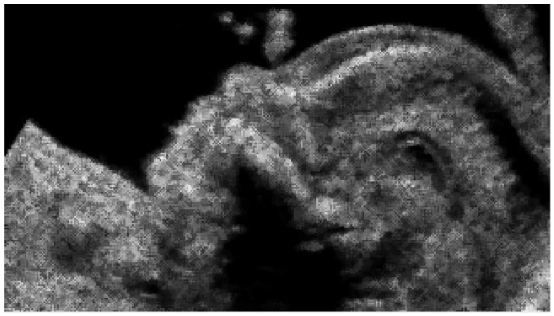

(I) HMF

(J) Proposed Method

Fig6.3 (A), (B), (C), (D), (E), (F), (G), (H), (I) and (J) original and noisy images and images filtered DsFca, DsFls, DsFg, SRAD , Wavelet, Median, Hybrid Median Filter and proposed method Modified Hybrid Median Filter respectively Results of **Fetal** despeckled by mentioned filter on multiplication noise (**σn=0.5**)

Table 6.2: Image quality evaluation metrics computed for the **fetal** (**σn**=0.5) at statistical measurement of SNR ,RSME,PSNR,UIQI and SSIM for different filter types .

Filter	RMSE	SNR	PSNR	UIQI	SSIM
DsFls	30.2168	11.7264	21.5361	0.3900	0.4781
DsFca	26.9500	12.7378	22.5299	0.4601	0.5421
DsFg	38.3113	9.9559	19.4745	0.4730	0.4821
SRAD	23.6270	13.8603	23.5123	0.5585	0.6221
Wavelet	29.6832	11.8939	21.6909	0.5482	0.6164
Med	24.0367	13.4569	23.5236	0.5971	0.6550
HMF	24.6512	13.3293	23.3043	0.6533	0.6945
Proposed Method	**22.3094**	**14.5567**	**24.2268**	**0.6989**	**0.7216**

Bold number indicates the best values.

*signal-to-noise ratio (SNR), root mean square error (RSME) peak-to-noise ratio (PSNR), Universal Image Quality Index(UIQI), structural similarity index (SSIM).

Figure 6.4: Performance analysis graph to image quality evaluation metric for **fetal** image (noise **σn** =0.5)

(A) Original image

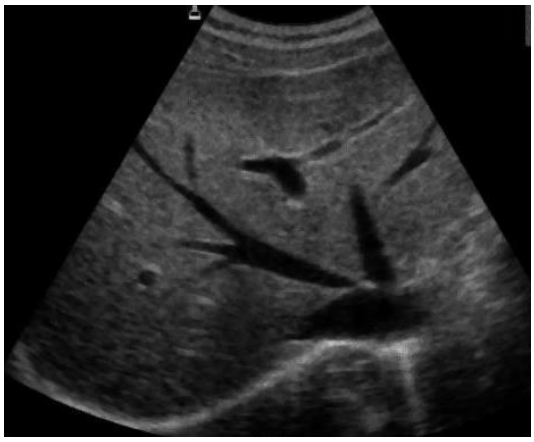

(B) Noisy image

(C) DsFca

(D) DsFls

(E) DsFg

(F) SRAD

(G) Wavelet

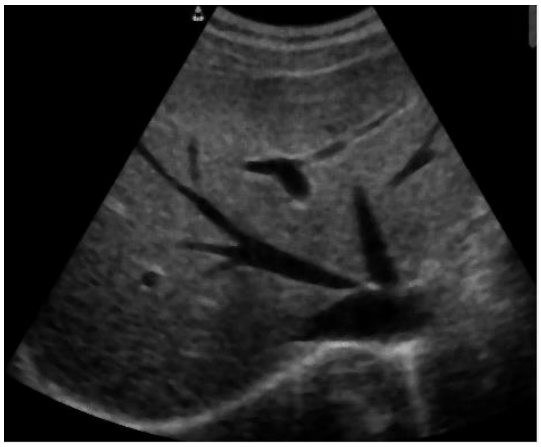

(H) Median

(I) HMF

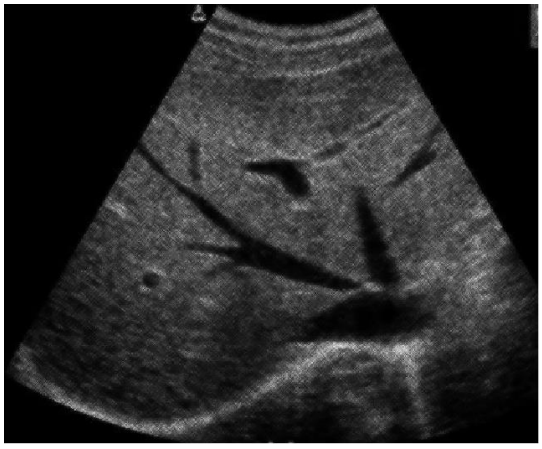

(J) Proposed Method

Figure 6.5 (A), (B), (C), (D), (E), (F), (G), (H), (I) and (J) original and noisy images and images by DsFca, DsFls, DsFg, SRAD , Wavelet, Median, Hybrid Median Filter and proposed method Modified Hybrid Median Filter respectively Results of **Liver** despeckled by mentioned filter on multiplication noise (**σn=0.05**)

Table 6.3: Image quality evaluation metrics computed for the **liver (σn=0.05)** at statistical measurement of SNR ,RSME,PSNR,UIQI and SSIM for different filter types .

Filter	RMSE	SNR	PSNR	UIQI	SSIM
DsFca	27.9722	8.5821	22.1038	0.4764	0.6476
DsFla	23.5512	9.8862	23.5980	0.4553	0.6393
DsFg	19.3156	11.4022	25.3201	0.6326	0.7423
SRAD	21.4959	10.4000	24.3912	0.2811	0.6489
Wavelet	21.8998	10.3041	24.2295	0.5966	0.7196
MED	21.4767	10.3782	24.3990	0.6370	0.7519
HMF	18.5189	11.6035	25.6860	0.6487	0.7412
Proposed Method	**15.6620**	**13.2108**	**27.1414**	**0.7782**	**0.8454**

Bold number indicates the best values.

* signal-to-noise ratio (SNR), root mean square error (RSME) peak-to-noise ratio (PSNR), Universal Image Quality Index(UIQI), structural similarity index (SSIM).

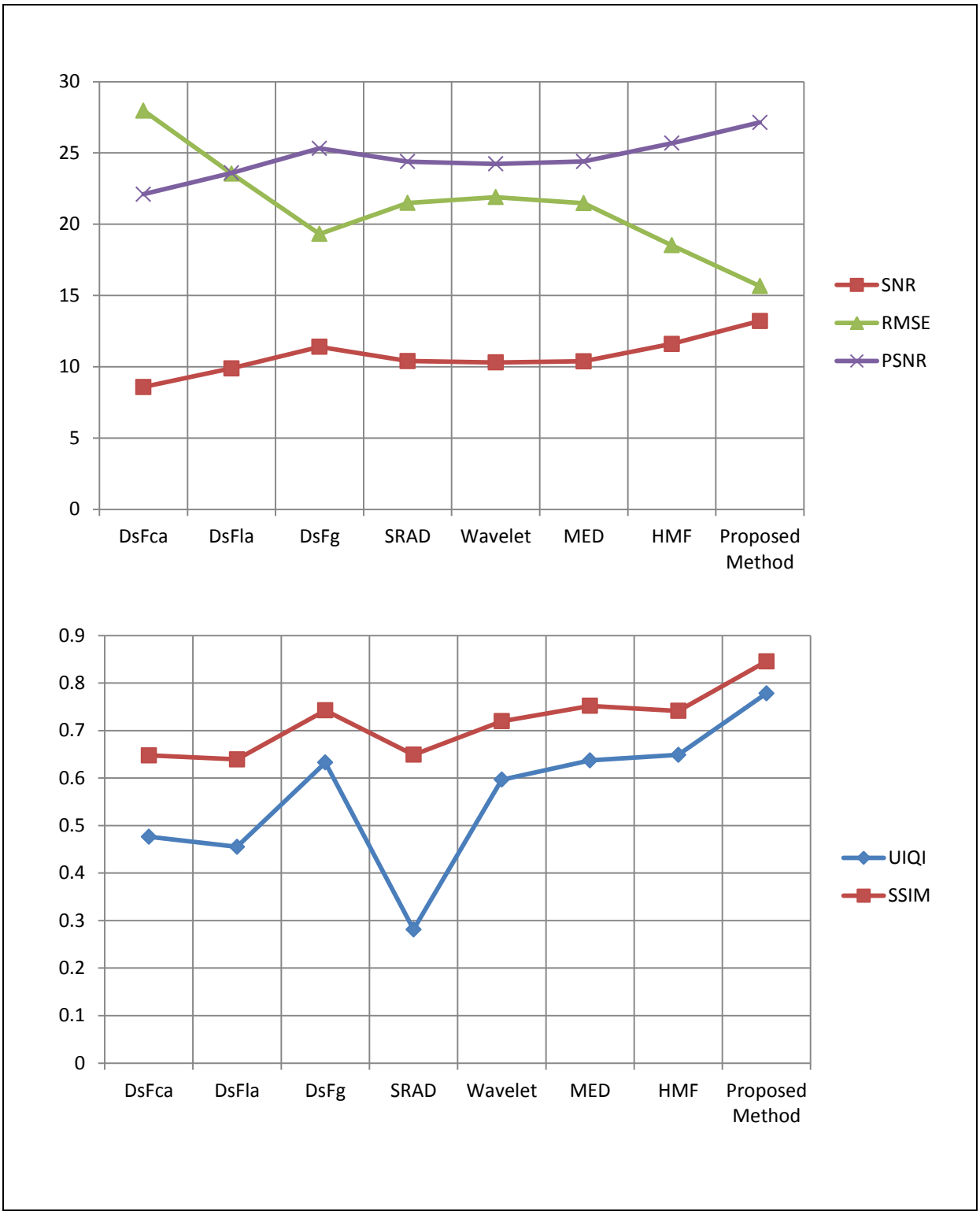

Figure 6.6: Performance analysis graph to image quality evaluation metric for **Liver** image (noise **σn** =0.05)

(A) Original image

(B) Noisy image

(C) DsFca

(D) DsFls

(E) DsFg

(F) SRAD

(G) Wavelet

(H) Median

(I) HMF

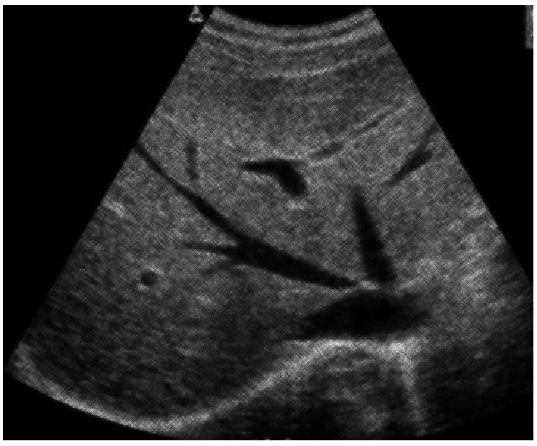

(J) Proposed Method

Figure 6.7 (A), (B), (C), (D), (E), (F), (G), (H), (I) and (J) original and noisy images and images filtered by DsFca, DsFls, DsFg, SRAD , Wavelet, Median, Hybrid Median Filter and proposed method Modified Hybrid Median Filter respectively Results of **Liver** despeckled by mentioned filter on multiplication noise (**σn=0.5**)

Table6. 4: Image quality evaluation metrics computed for the **liver** (**σn**=0.5) at statistical measurement of SNR ,RSME,PSNR,UIQI and SSIM for different filter types .

Felter	RMSE	SNR	PSNR	UIQI	SSIM
DsFca	27.5521	9.1114	22.2352	0.4675	0.6259
DsFls	23.1561	10.4485	23.7450	0.4701	0.6308
DsFg	34.0581	7.1155	20.3938	0.4275	0.4639
SRAD	28.1248	8.5597	22.0565	0.4428	0.6130
Wavelet	26.6301	8.8013	22.5309	0.4807	0.6206
MED	22.9977	9.7731	23.8046	0.5785	0.7027
HMF	28.9042	8.1029	21.8191	0.5367	0.6409
Proposed Method	**16.2052**	**13.1509**	**26.8452**	**0.6828**	**0.7461**

Bold number indicates the best values.

* signal-to-noise ratio (SNR), root mean square error (RSME) peak-to-noise ratio (PSNR), Universal Image Quality Index(UIQI), structural similarity index (SSIM).

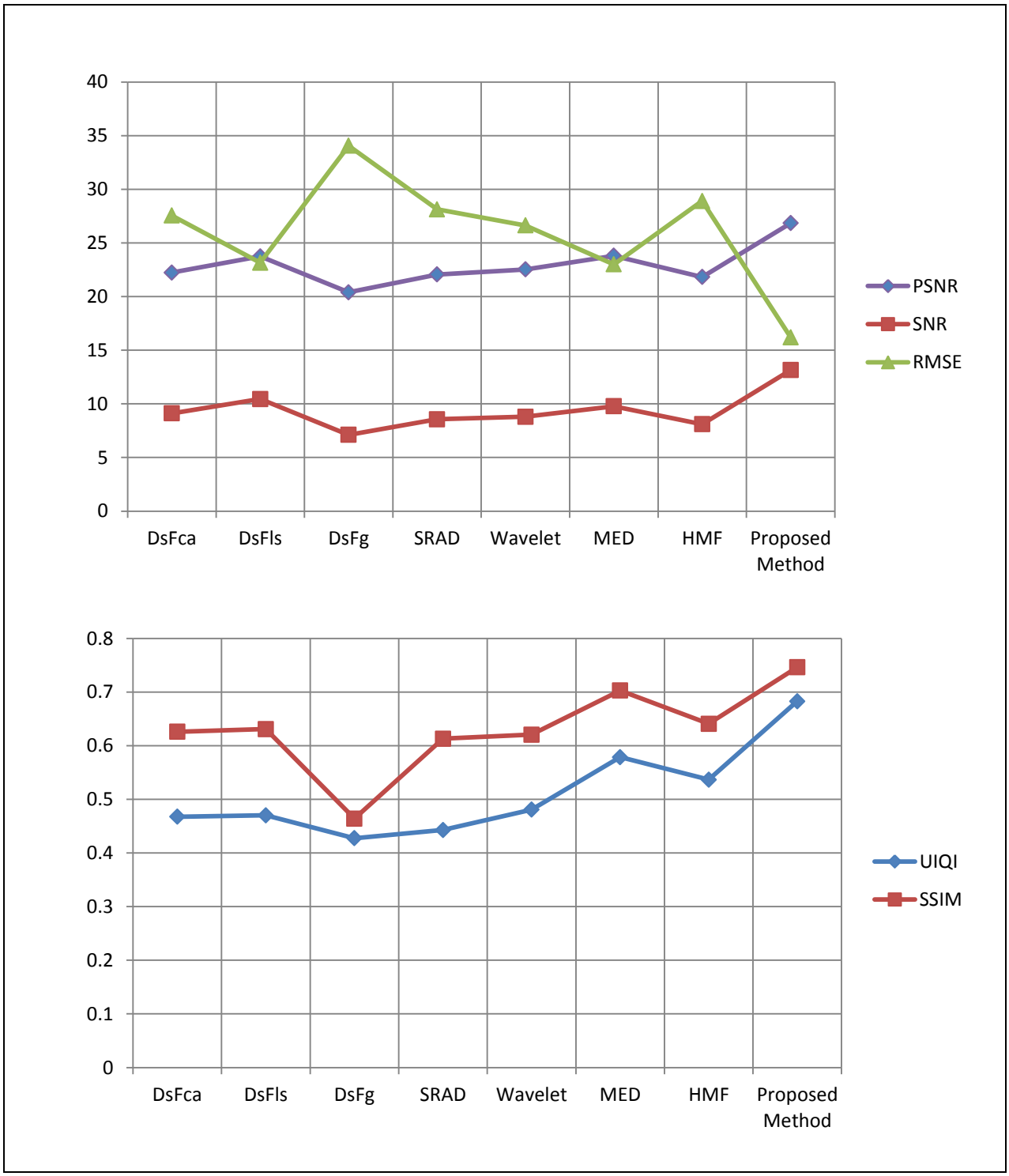

Figure 6.8: Performance analysis graph to image quality evaluation metric for **Liver** image (noise **σn** =0.5)

Most importantly, a despeckle filtering analysis and evaluation framework is proposed for selecting the most appropriate filter or filters for the images under investigation. The filters can be further developed and evaluated at a larger scale, texture analysis, image quality evaluation metrics, and visual evaluation by experts.

From figures 6.1,6.3,6.5,6.7, show an ultrasound image (A) with noisy (B) and the despeckled images, in (C) can see that, the linear scaling gray level filter (DsFca) has high degree of blurring and was affect on gray level, because it is compute the mean of all pixels whose difference in the gray level with the intensity(the middle pixel in the moving window) is lower than or equal to a given threshold, (D) Show the result obtained by liner scaling (DsFls) filter scales the pixel intensities by finding the maximum and the minimum gray-level values in every moving window, and then replaces the middle pixel with the average of them also give blurred image. (E) although the result obtained by geometric despeckle filter (DsFg) given poor performance for removing the speckle noise from the ultrasound image, it is lead to increasing the contrast significantly of the image. (F) show the result of speckle reducing anisotropic diffusion filtering(srad), it is better for preserves the edges as a comparison with the other despeckle filtering techniques and subjectively has good result, and referred to evaluated metrics, it was also given bad results, (G) the result through wavelet despeckle filtering perceived that it's moderate in order of variance decreasing but execute to decrease the contrast (H) show the result obtained by median despeckle filter, which don't able to remove the speckle and produced blurred edges in the filtered image .figure(I) show the result of hybrid median filter (HMF) given better edge preserving characteristics than normal median filter.

From table 6.1,6.2,6.3,6.4, tabulates the image quality evaluation contains the metric result of filters under study, The best visual results were obtained for the filters DsFg, SRAD, HMF and Median filter because with higher SNR and PSNR and lower RMSE and Best values for the SSlM and UIQI, but visually, smoothed the image. Loosing subtle details are been observed.

In same mentioned tables and figures, can show that the **modified hybrid median** filter has best performances over all despeckling filters, due to the median filter ability of modifying pixels without affecting by noise moreover The best way for noise reduction is to process the image by its individual pixels based on its neighbours such as in Median filter. The max instruction return the maximum value within selected window which affects the brightness of image. As for the mean filter, it is employed to change each pixel's value with mean value of its neighbours. If an image is corrupted with low variance, it works better for additive noise. As the noise level increases, its performance deteriorate by showing blurring effects.

the performance of despeckled filters are depended on image's features and quantity of speckle noise which applied on image, this clear in Table 6.2,6.4 shows that even the noise level increases, the proposed method still gives better results than other existing methods.

Evaluation step:

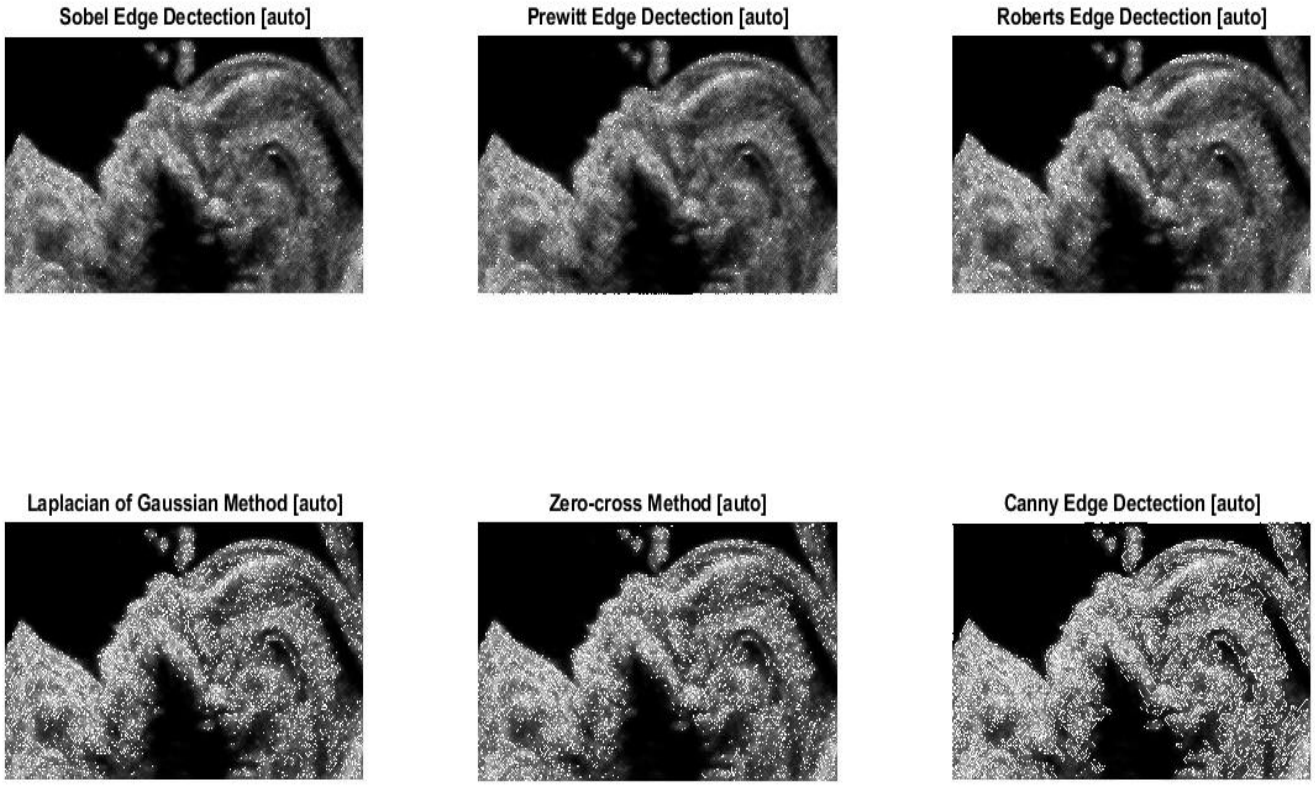

Result of edge detection

Figure 6.9 Result of various edge detection operators for despeckling **fetal** image MHMF (**σn**= 0.05).

Table:6,5 Image quality evaluation metrics computed for the **Fetal** image resulted from Modified hybrid median filter edge detection operators (**σn** =0.05) at statistical measurement of SNR ,RSME,PSNR,UIQI, SSIM and EPF.

Felter	RMSE	SNR	PSNR	UIQI	SSIM	EPF
Sobel	36.9917	10.5221	19.7789	0.5497	0.5918	0.8204
Prewitt	**23.8719**	**14.0275**	**23.5833**	**0.6169**	**0.6390**	**0.9168**
Roberts	31.4908	11.8830	21.1774	0.5526	0.5832	0.8735
Log	46.8324	9.22611	17.7301	0.3998	0.4285	0.8166
Zero-cross	48.4531	8.9169	17.4346	0.4039	0.4360	0.7950
Canny	58.5502	7.8518	15.7905	0.3244	0.3547	0.7733

Bold number indicates the best values.

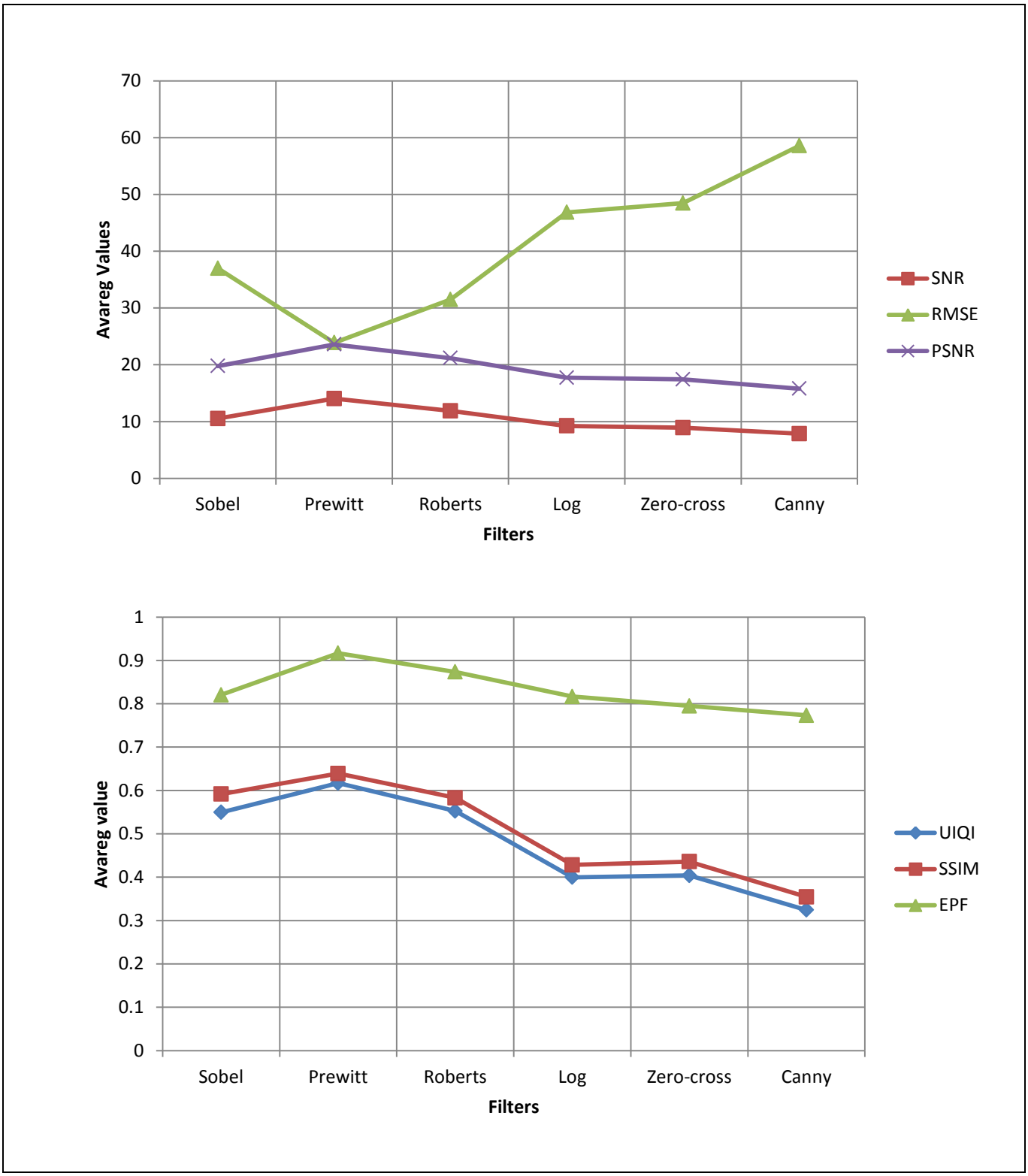

Figure 6.10: Performance analysis graph to image quality evaluation metric for **fetal** image (noise **σn =0.05**)

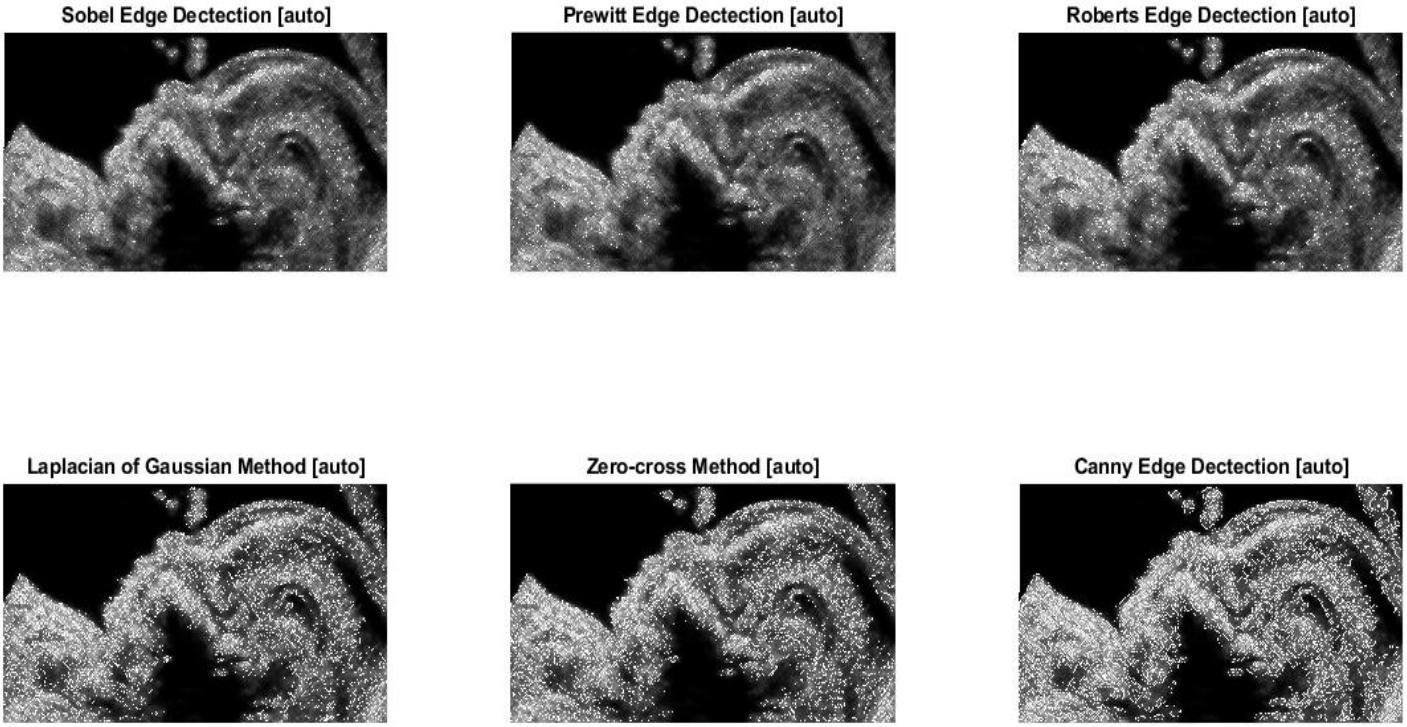

Figure 6.11: Result of various edge detection operators for despeckling **Fetal** image MHMF (**σn**= 0.5)

Table:6.6 Image quality evaluation metrics computed for the **Fetal** image resulted from Modified hybrid median filter edge detection operators (**σ =0.5**) at statistical measurement of SNR ,RSME,PSNR,UIQI,SSIM and EPF.

Felter	RMSE	SNR	PSNR	UIQI	SSIM	EPF
Sobel	36.8729	10.6019	19.8069	0.5611	0.5945	0.8288
Prewitt	**30.7235**	**12.0191**	**21.3916**	**0.58714**	**0.6157**	**0.8728**
Roberts	33.9615	11.3335	20.5213	0.5005	0.5371	0.8608
Log	52.4996	8.3970	16.7379	0.3426	0.3792	0.7759
Zero-cross	48.9189	8.9087	17.3515	0.3690	0.3974	0.8017
Canny	61.8975	7.4107	15.3076	0.2583	0.3066	0.7364

Bold number indicates the best values.

* signal-to-noise ratio (SNR), root mean square error (RSME) peak-to-noise ratio (PSNR), Universal Image Quality Index(UIQI), Structural Similarity Index (SSIM), Edge Preservation Factor(EPF).

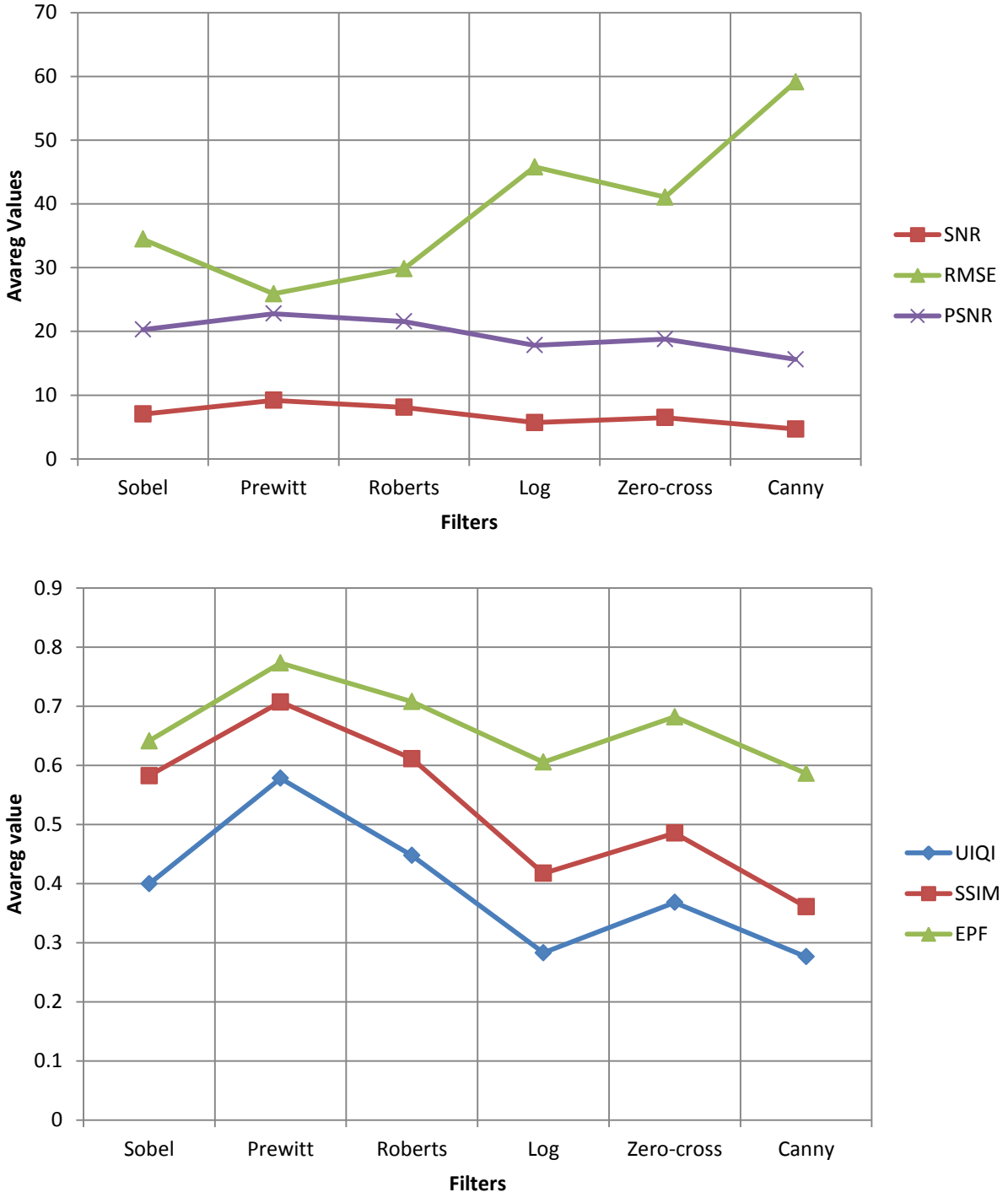

Figure 6.14: Performance analysis graph to image quality evaluation metric for **liver** image (noise **σn =0.05**)

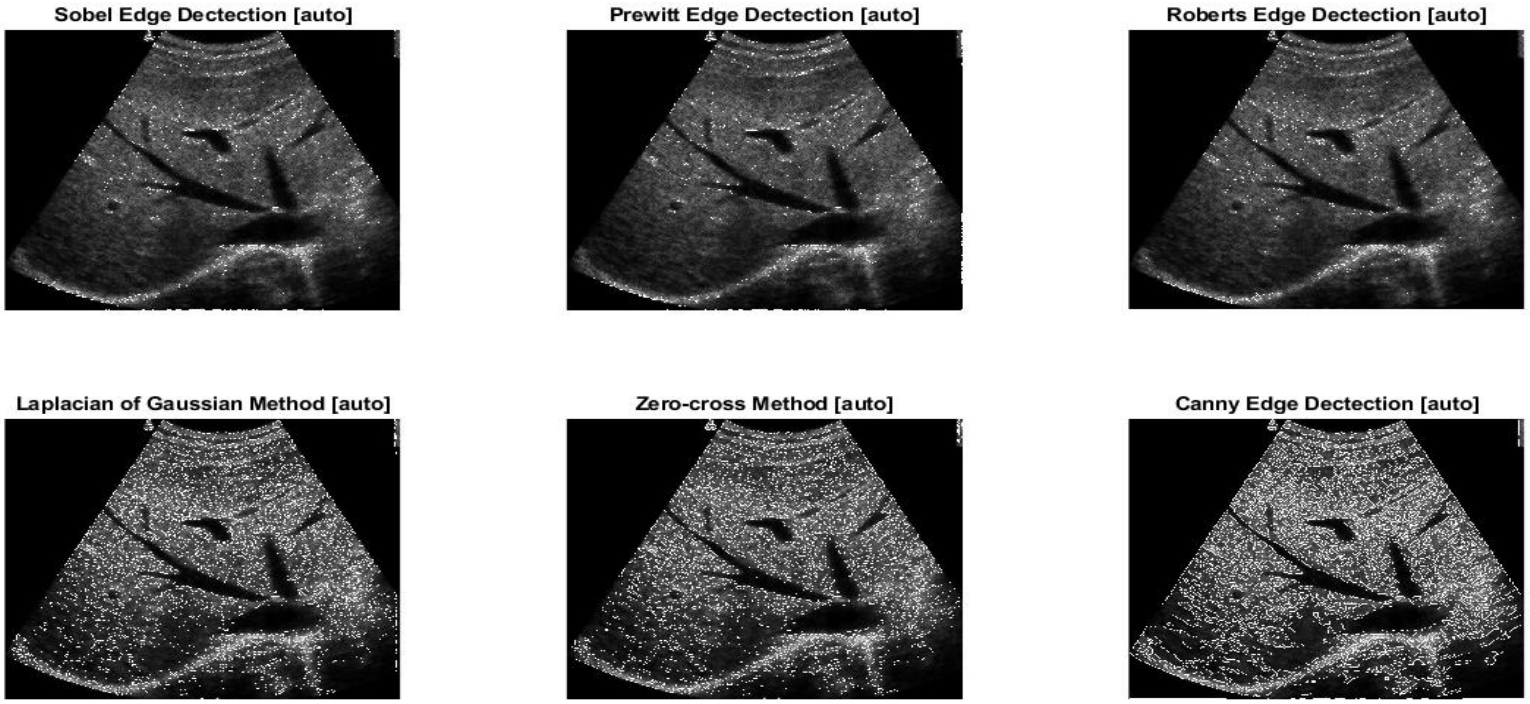

Figure: 6.15 Result of various edge detection operators for despeckling **Liver** image MHMF (**σn**= 0.5)

Table: 6.8 Image quality evaluation metrics computed for the **Liver** image resulted from Modified Hybrid Median filter edge detection operators (**σn =0. 5**) at statistical measurement of SNR, RSME, PSNR, UIQI, SSIM and EPF.

Felter	RMSE	SNR	PSNR	UIQI	SSIM	EPF
Sobel	46.2827	5.3537	17.7299	0.3392	0.4973	0.5300
Prewitt	**25.2423**	**9.7459**	**22.9957**	**0.5882**	**0.6650**	**0.8250**
Roberts	33.3145	7.6577	20.5856	0.4604	0.5794	0.7193
Log	55.5088	4.9802	16.1511	0.2893	0.3810	0.6071
Zero-cross	54.9874	5.0365	16.2330	0.2905	0.3832	0.6140
Canny	64.7868	4.4710	14.8085	0.2707	0.3464	0.6153

Bold number indicates the best values.

* signal-to-noise ratio (SNR), root mean square error (RSME) peak-to-noise ratio (PSNR), Universal Image Quality Index(UIQI), Structural Similarity Index (SSIM), Edge Preservation Factor(EPF).

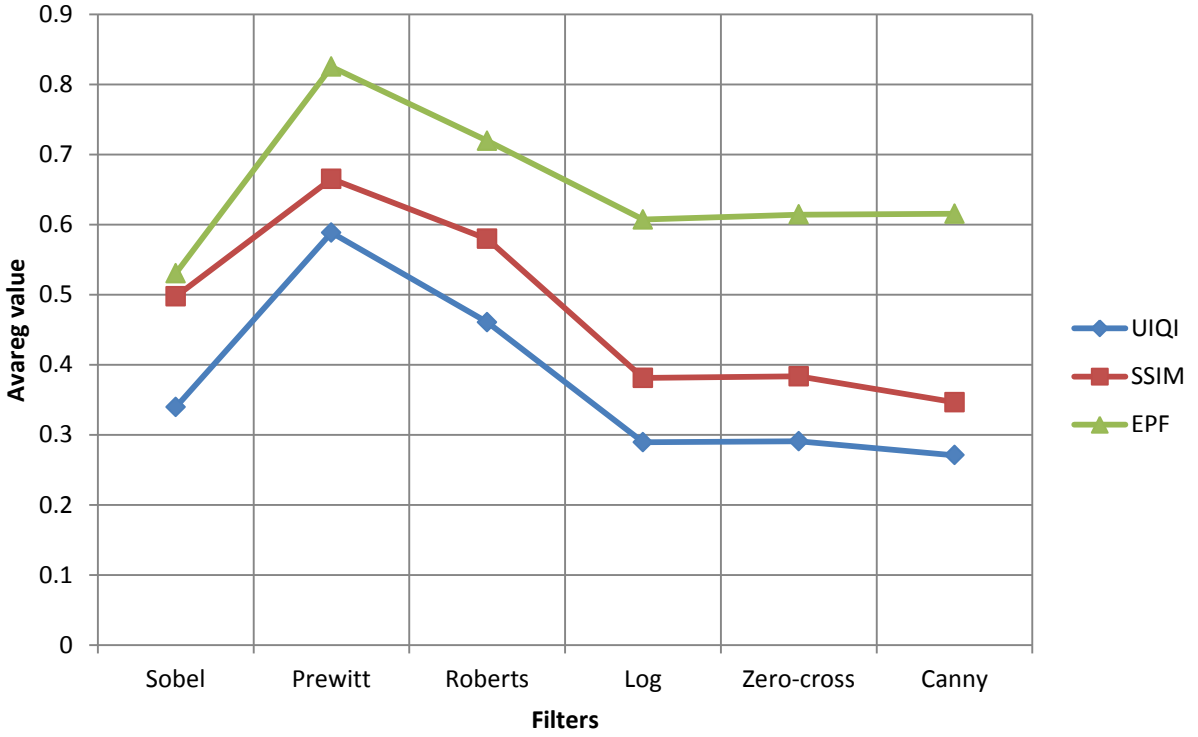

Figure 6.16: Performance analysis graph to image quality evaluation metric for **liver** image

(noise **σn =0.5**)

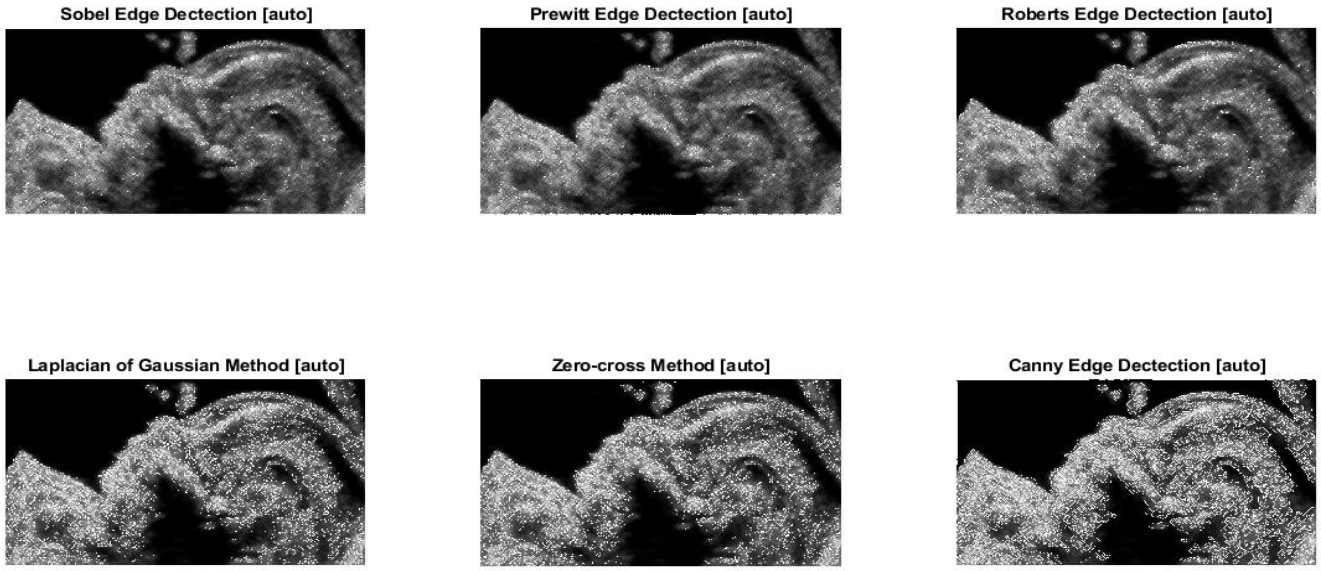

Figure: 6.17 Result of various edge detection operators for despeckling **Fetal** image using HMF

Table: 6.9 Image quality evaluation metrics computed for the **fetal** image resulted from Hybrid Median filter edge detection operators (**σn =0.05**) at statistical measurement UIQI, SSIM and EPF.

Felter	UIQI	SSIM	EPF
Sobel	**0.5270**	**0.9958**	**0.8398**
Prewitt	0.1418	0.2384	0.6044
Roberts	0.1321	0.2405	0.5982
Log	0.1295	0.2322	0.5700
Zero-cross	0.0452	0.9958	0.8365
Canny	0.1340	0.2147	0.5788

Bold number indicates the best values.

* Universal Image Quality Index (UIQI), Structural Similarity Index (SSIM), Edge Preservation Factor (EPF).

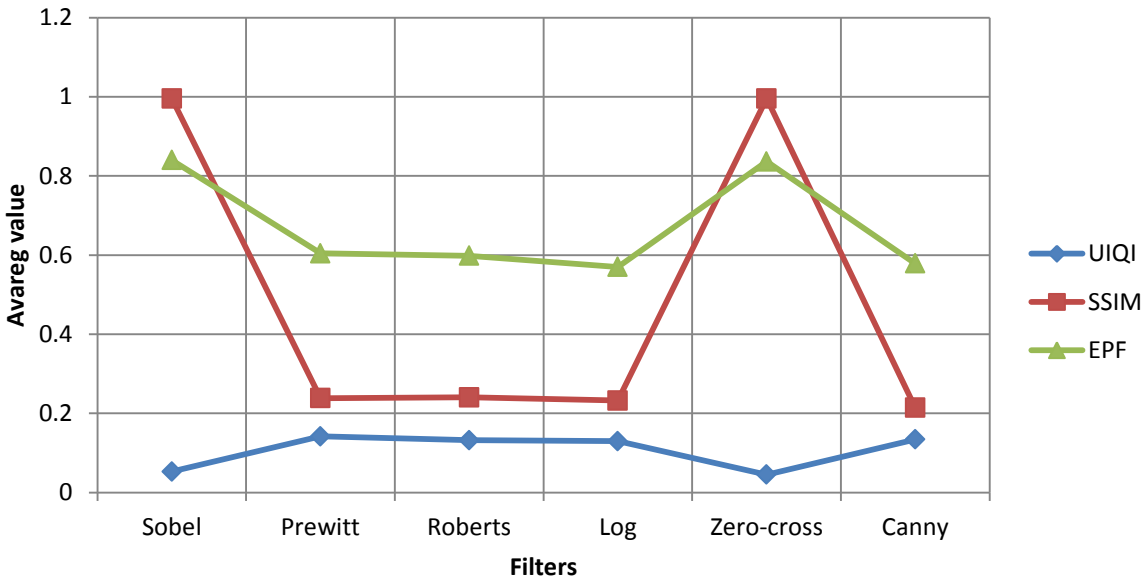

Figure 6.18: Performance analysis graph to image quality evaluation metric for **fetal** image

(noise **σn =0.05**)

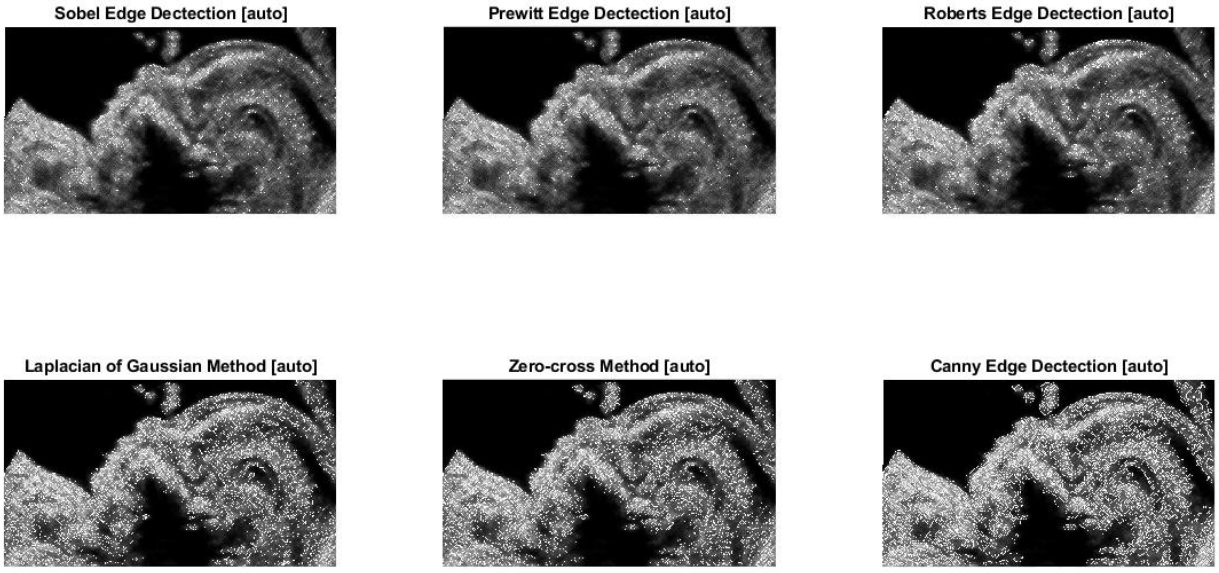

Figure: 6.19 Result of various edge detection operators for despeckling **fetal** image using HMF

Table: 6.10 Image quality evaluation metrics computed for the **fetal** image resulted from Hybrid Median filter edge detection operators (**σn =0. 5**) at statistical measurement UIQI, SSIM and EPF.

Felter	UIQI	SSIM	EPF
Sobel	0.1316	0.2386	0.6072
Prewitt	0.1345	0.2355	0.6139
Roberts	0.1337	0.2339	0.6086
Log	0.1340	0.2258	0.5845
Zero-cross	0.1335	0.2265	0.5909
Canny	**0.6811**	**0.9953**	**0.8613**

Bold number indicates the best values.

* Universal Image Quality Index (UIQI), Structural Similarity Index (SSIM), Edge Preservation Factor (EPF).

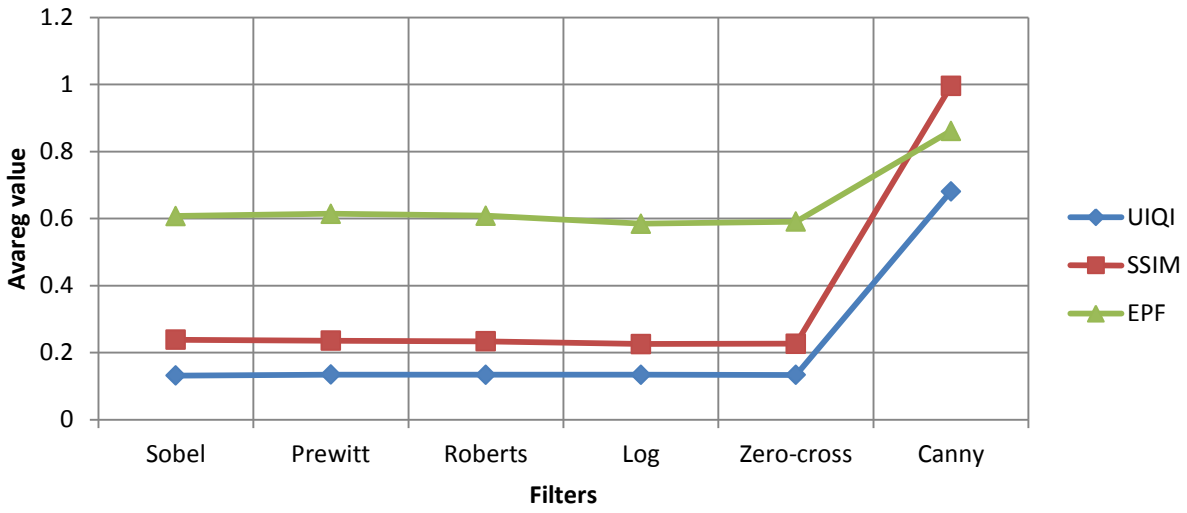

Figure 6.20: Performance analysis graph to image quality evaluation metric for **fetal** image

(noise **σn =0.05**)

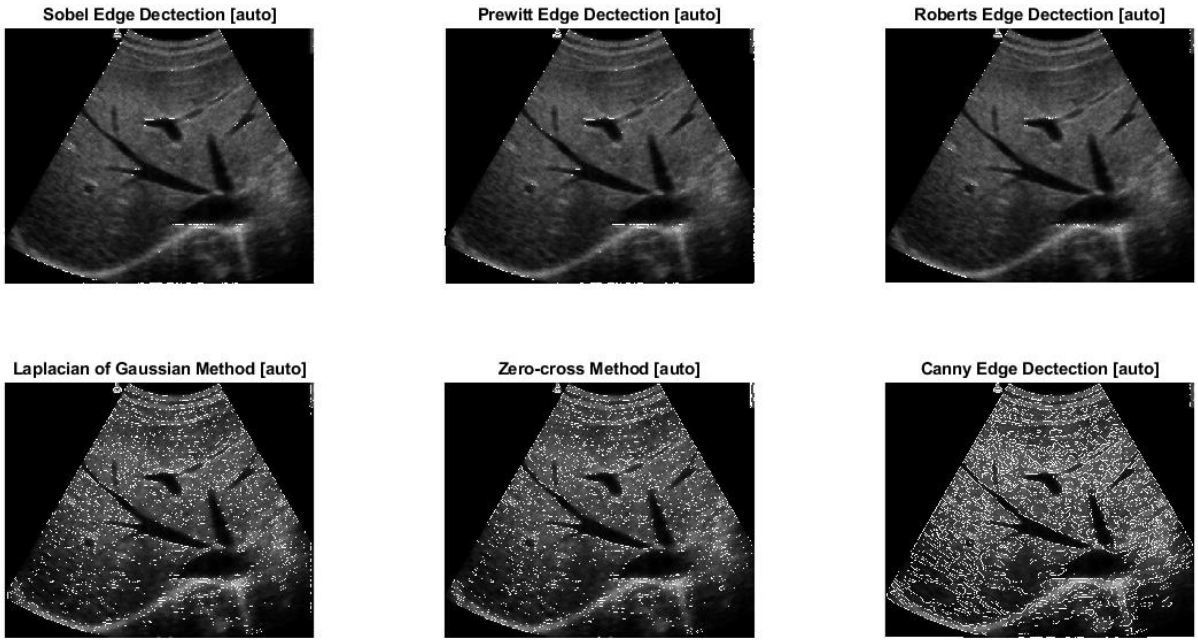

Figure: 6.21 Result of various edge detection operators for despeckling **liver** image using HMF

Table: 6.11 Image quality evaluation metrics computed for the **liver** image resulted from Hybrid Median filter edge detection operators (**σn =0. 05**) at statistical measurement UIQI, SSIM and EPF.

Felter	UIQI	SSIM	EPF
Sobel	0.1819	0.2571	0.5466
Prewitt	0.1814	0.2581	0.5129
Roberts	0.1824	**0.2583**	**0.5871**
Log	0.1700	0.2434	0.4777
Zero-cross	0.1814	0.2382	0.5173
Canny	**0.1830**	0.2325	0.5263

Bold number indicates the best values.

* Universal Image Quality Index (UIQI), Structural Similarity Index (SSIM), Edge Preservation Factor (EPF).

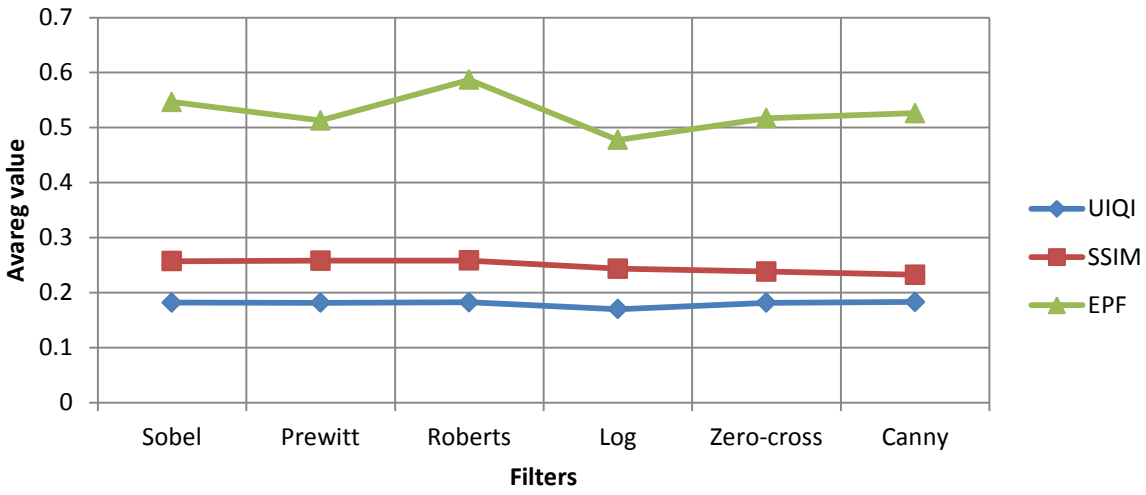

Figure 6.22: Performance analysis graph to image quality evaluation metric for **liver** image

(noise **σn =0.05**)

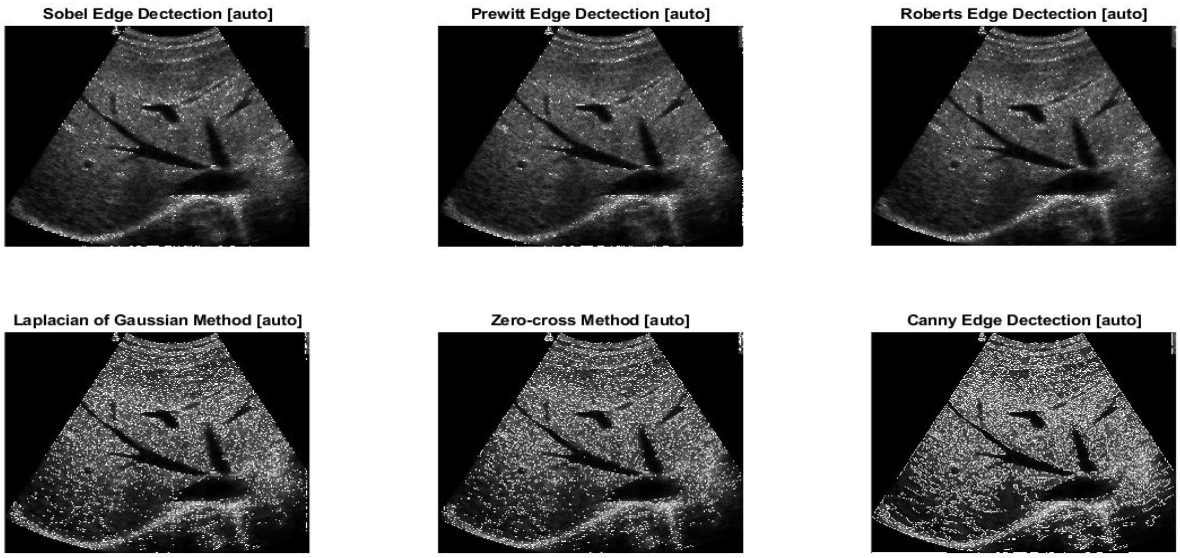

Figure: 6.23 Result of various edge detection operators for despeckling **liver** image using HMF

Table: 6.12 Image quality evaluation metrics computed for the **liver** image resulted from Hybrid Median filter edge detection operators (**σn =0.5**) at statistical measurement UIQI, SSIM and EPF.

Felter	UIQI	SSIM	EPF
Sobel	0.1706	0.2666	0.5225
Prewitt	0.1760	0.2676	0.5994
Roberts	0.1632	0.2666	0.4130
Log	0.1738	0.2501	0.5204
Zero-cross	0.1721	0.2529	0.5111
Canny	**0.5529**	**0.9946**	**0.8460**

Bold number indicates the best values.

* Universal Image Quality Index (UIQI), Structural Similarity Index (SSIM), Edge Preservation Factor (EPF).

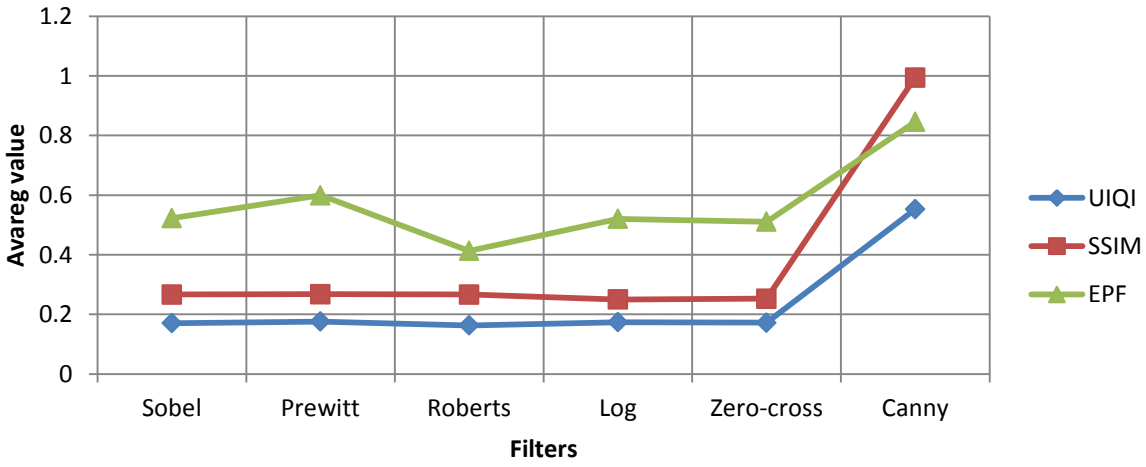

Figure 6.24: Performance analysis graph to image quality evaluation metric for **liver** image

(noise **σn =0.5**)

By modify the hybrid median filter, this gives better edge preserving characteristics than hybrid median filter, which can shows in figure 6.9,6.11,6.13,6.15, and table 6.5, 6.6, 6.7, 6.8 that tabulates the result of edge detection method when using the proposed filter as despeckle filter. From tables Prewitt filter gives best result while the Canny filter gives more details.

The combination between MHMD and Prewitt increase the brightness of image by taking the max value, as shown in the image quality metrics EPF, so the result is better than normal hybrid median.

CHAPTER SEVEN

7.1 Conclusion:

US is relatively inexpensive, portable, safe, and real time in nature. These characteristics, and continued improvements in image quality and resolution have expanded the use of US to many areas in medicine beyond traditional diagnostic imaging applications

In diagnosis of diseases Ultrasonic devices are frequently used by healthcare professionals. The main problem during diagnosis is the distortion of visual signals obtained which is due to the consequence of the coherent of nature of the wave transmitted. These distortions are termed as speckle N Arbitration between the perpetuation of useful diagnostic information and noise suppression must be treasured in medical images.

The present study focuses on proposing a technique to reduce speckle noise from ultrasonic images.

Here the proposed method for speckle noise reduction in ultrasound image with edge detection is (modified hybrid median filter) a modified version of hybrid median filter to get best result and preserve the edges of image than the normal one.

In the evaluation in several image applications including image interpolation and impulsive noise reduction, both quantitative and qualitative comparison showed that the MHMF exhibit improved performance and merit further attention.

The experimental results show that proposed filter yield better SNR, PSNR, RSME, SSIM, UIQI and EPF in comparison with other despeckle filters and HMF at moderate as well as high noise levels. The performance of proposed filter is studied under moderate and high standard deviation. From results, it is observed that the proposed filter perform well in terms of noise suppression and edge preservation. The subjective evaluation is done by representing the visual results of different filters at speckle noise.

The proposed method takes full advantage of combine and filters modification, to reduce speckle noise, not only to enhance those filters but to obtain filters which

capable to get a good result referred to quality evaluation metric. While, subjectively, can be used in diagnostic and therapeutic terms.

7.2 Recommendation and Future work:

- Assess window size to work in large image.
- Estimate speckle noise level within original image.
- Use different standers deviation of speckle noise as range
- Use medical ultrasonic image with structural feature to measure filter ability to detect borders.
- Use stander image to evaluate filter ability to preserve edges.
- Increase images number to evaluate filter performance.

In future work, the implementation of proposed filter in Neutrosophic domain is in progress. Neutrosophy is a branch of philosophy, which includes four fields: philosophy, logics, set theory, and probability/statistics. It can solve some problems that cannot be solved by the fuzzy logic

In the field of image denoising, more researches are needed to develop very effective filters. As the edge detection is affected by threshold level, so the selection of the threshold value should be more related to image content.

References:

1. Alisha P B , Gnana Sheela K. Image Denoising Techniques-An Overview. *Journal of Electronics and Communication Engineering*. (2016, 2).
2. Bandyopadhyay, S. K.. Edge Detection in Brain Images. *International Journal of Computer Science and Information Technologies, 2*. (2011, Jun)
3. K. Karthikeyan , Dr. C. Chandrasekar,. "Speckle Noise Reduction of Medical Ultrasound Images using Bayesshrink Wavelet Threshold. *IEEE*. (2012, MAY).
4. S. Sudha , G. R. Suresh and R. Sukanesh. Speckle Noise Reduction in Ultrasound Images Using Context-based Adaptive Wavelet Thresholding. *IETE JOURNAL OF RESEARCH*. (2009, MAY).
5. MR. HITESH S. ASARI, 2ASS.PROF. AMI SHAH,A.D. Patel institute and Technologey, " *A Research Paper On Reducion Of Speckle Noise In Ultrasound Imaging Using Wavelet And Contour let Transform*", journal of information, knowledge and research in electronics and communication engineering , nov 2013
6. Jens E. Wilhjelm, Andreas Illum, Martin Kristensson and Ole Trier Andersen, "*Medical diagnostic ultrasound- physical principles and imaging*",Biomedical Engineering, DTU ElektroTechnical University of Denmark (Ver. 3.1, 2 October 2013) ©by J. E. Wilhjelm.
7. institute of physics publishing physics in medicine and biology, "*Ultrasound imaging*", Phys. Med. Biol. 51 (2006).
8. https://www.sprawlsultrasound.org /production and interactions,10 -2015.
9. Thomas M. Deserno, "*Fundamentals of Biomedical Image Processing*" springer, 2015.
10. S.Kalaivani Narayanan and R.S.D.Wahidabanu"*A View on Despeckling in Ultrasound Imaging*",International Journal of Signal Processing, Image Processing and Pattern Recognition,Vol. 2, No.3, September 2009.
11. R.vanithamani 1, G.umamaheswari2, M.ezhilarasi3,"*Modified Hybrid Median Filter for Effective Speckle Reduction in Ultrasound Images*"(2010)
12. Christos P. Loizou, Constantinos S. Pattichis, Robert S. H. Istepanian, "*Comparative Evaluation of Despeckle Filtering In Ultrasound Imaging of the Carotid Artery*" (october 2005).
13. Vaishali Kumbhakarna MPHIL (Computer Science)III Sem, Vijaya R.Patil MPHIL (Computer Science)III Sem,Dr.Seema Kawathekar(Asst.Prof), Review on Speckle Noise Reduction Techniques for Medical Ultrasound Image Processing , International Journal of Computer Techniques Volume 2 Issue 1, (2015).

14. Christos P. Loizou and Constantinos S. Pattichis , “Despeckle Filtering Algorithms and Software for Ultrasound Imaging”, Copyright © by Morgan & Claypool (2008).
15. Dhrub Kumar , Maitreyee Dutta , Parveen Lehana , “*A Comparative Analysis of Different Wavelets for Enhancing Medical Ultrasound Images*” , March 2013
16. Jyoti Jaybhay and Rajveer Shastri," *A STUDY OF SPECKLE NOISE REDUCTION FILTERS Signal & Image Processing* ": An International Journal (SIPIJ) Vol.6, No.3, (June 2015).
17. Mohanapreethi, Dr. V. Srinivasa Raghavan, “*A. Multiresolution Based Hybrid Filtering Technique for Despeckling Ultrasound Images*”, (May-Jun. 2014).
18. Yusra A. Y. Al-Najjar, Dr. Der Chen Soong," *Comparison of Image Quality Assessment: PSNR, HVS, SSIM, UIQI" International Journal of Scientific & Engineering Research*", Volume 3, Issue 8, August-2012
19. R. Vanithamani .G.Umamaheswari, “*Performance Analysis of Filters for Speckle Reduction in Medical Ultrasound Images*” International Journal of Computer Applications (0975 –8887)Volume 12–No.6, December 2010
20. Poobathy D,Dr. RManicka Chezian," *A Survey on Edge Detection Algorithms*", nternational Journal of Electrical Electronics & Computer Science Engineering Volume 4, Issue 5(October, 2017)
21. Harpreet Singh, Er. MandeepKaur, " *A Review: Sobel Canny Hybrid Theoretical Approach & LOG Edge Detection Techniques for Digital Image*". International Journal of Computer Science & Engineering Technology, Vol. 6 No. 02 Feb 2015.
22. Computed Tomography (CT) -Head, Radiology Information, Copyright © Feb-12-2014.
23. ..Canny,"*A Computational Approach to Edge Detection*", IEEE PAMI, VOL.8,NO.6,Novermber 1986.
24. V.S. Nalwa and T.S. Binford, "*On Detecting Edge"*, IEEE Trans. PAMI.VOL. 8,NO. 6, pp699-714, November 1986
25. Raman Maini & Dr. Himanshu Aggarwal," *Study and Comparison of Various Image Edge Detection Techniques*", International Journal of Image Processing (IJIP), Volume (3) : Issue (1), Patiala-147002(Punjab), India
26. Deepa and M.Suganthi ,"*Performance Evaluation of Various Denoising Filters for Medical Image*",(IJCSIT) International Journal of Computer Science and Information Technologies, Vol. 5 (3) , 2014, 4205-4209

27. - Muthukrishnan.R and M.Radha," *edge detection techniques for image segmentation*", International Journal of Computer Science & Information Technology (IJCSIT) Vol 3, No 6, Dec 2011.